Analysis and numerical methods for nonlocal models

by

Ilyas Aderogba Mustapha

B.S., University of Ibadan, 2015

M.S., African Institute for Mathematical Sciences, 2018

M.S., Kansas State University, 2021

AN ABSTRACT OF A DISSERTATION

submitted in partial fulfillment of the
requirements for the degree

DOCTOR OF PHILOSOPHY

Department of Mathematics
College of Arts and Sciences

KANSAS STATE UNIVERSITY
Manhattan, Kansas

2025

Abstract

This dissertation addresses the regularity of solutions for nonlocal diffusion equations over the space of periodic distributions. The spatial operator for the nonlocal diffusion equation is given by a nonlocal Laplace operator with a compactly supported integral kernel. We follow a unified approach based on the Fourier multipliers of the nonlocal Laplace operator, which allows the study of regular and distributional solutions of the nonlocal diffusion equation, as well as integrable and singular kernels, in any spatial dimension. In addition, the results extend beyond operators with singular kernels to nonlocal super-diffusion operators. We present results on the spatial and temporal regularity of solutions in terms of the regularity of the initial data or the diffusion source term. Moreover, solutions of the nonlocal diffusion equation are shown to converge to the solution of the classical diffusion equation for two types of limits: as the spatial nonlocality vanishes or as the singularity of the integral kernel approaches a certain critical singularity that depends on the spatial dimension. Furthermore, we show that, for the case of integrable kernels, discontinuities in the initial data propagate and persist in the solution of the nonlocal diffusion equation. The magnitude of a jump discontinuity is shown to decay over time.

In addition, we present a spectral numerical method for nonlocal equations on bounded domains. These spectral solvers exploit the fact that integration in the nonlocal formulation transforms into multiplication in Fourier space and that nonlocality is decoupled from the grid size. Our approach extends the spectral solvers developed in [1] for periodic domains by incorporating the two-dimensional Fourier Continuation (2D-FC) algorithm introduced in [2]. We evaluate the performance of the proposed methods on two-dimensional nonlocal Poisson and nonlocal diffusion equations defined on bounded domains. While the regularity of solutions to these equations in bounded settings remains an open problem, we conduct numerical experiments to explore this issue, particularly focusing on studying discontinuities.

Analysis and numerical methods for nonlocal models

by

Ilyas Aderogba Mustapha

B.S., University of Ibadan, 2015

M.S., African Institute for Mathematical Sciences, 2018

M.S., Kansas State University, 2021

A DISSERTATION

submitted in partial fulfillment of the
requirements for the degree

DOCTOR OF PHILOSOPHY

Department of Mathematics
College of Arts and Science

KANSAS STATE UNIVERSITY
Manhattan, Kansas

2025

Approved by:

Major Professor
Bacim Alali

Copyright

Abstract

This dissertation addresses the regularity of solutions for nonlocal diffusion equations over the space of periodic distributions. The spatial operator for the nonlocal diffusion equation is given by a nonlocal Laplace operator with a compactly supported integral kernel. We follow a unified approach based on the Fourier multipliers of the nonlocal Laplace operator, which allows the study of regular and distributional solutions of the nonlocal diffusion equation, as well as integrable and singular kernels, in any spatial dimension. In addition, the results extend beyond operators with singular kernels to nonlocal super-diffusion operators. We present results on the spatial and temporal regularity of solutions in terms of the regularity of the initial data or the diffusion source term. Moreover, solutions of the nonlocal diffusion equation are shown to converge to the solution of the classical diffusion equation for two types of limits: as the spatial nonlocality vanishes or as the singularity of the integral kernel approaches a certain critical singularity that depends on the spatial dimension. Furthermore, we show that, for the case of integrable kernels, discontinuities in the initial data propagate and persist in the solution of the nonlocal diffusion equation. The magnitude of a jump discontinuity is shown to decay over time.

In addition, we present a spectral numerical method for nonlocal equations on bounded domains. These spectral solvers exploit the fact that integration in the nonlocal formulation transforms into multiplication in Fourier space and that nonlocality is decoupled from the grid size. Our approach extends the spectral solvers developed in [1] for periodic domains by incorporating the two-dimensional Fourier Continuation (2D-FC) algorithm introduced in [2]. We evaluate the performance of the proposed methods on two-dimensional nonlocal Poisson and nonlocal diffusion equations defined on bounded domains. While the regularity of solutions to these equations in bounded settings remains an open problem, we conduct numerical experiments to explore this issue, particularly focusing on studying discontinuities.

Table of Contents

List of Figures

List of Tables

Acknowledgments

Foremost, I am deeply grateful to God Almighty for His endless grace, mercy, and blessings he bestowed on me throughout this journey. It is by His will that I have come this far, and I recognize that every step of this journey has only been possible through His guidance and provision. I am thankful to Him for giving me the strength, patience, perseverance, and support I needed that helped me reach this milestone.

My deepest gratitude and heartfelt appreciation go to my advisor, Dr. Bacim Alali, for his unwavering support, guidance, and untiring efforts throughout this journey. His expertise, insightful feedback, and steady encouragement have been instrumental in refining my research. I am especially thankful for his patience, his words of encouragement, and his commitment to my academic and personal growth. I also extend my heartfelt thanks to the esteemed members of my committee, Dr. Nathan Albin, Dr. Lizaveta Ihnatsyeva, and Dr. Hayder Rasheed, whose insights and feedback have been invaluable.

Additionally, I am deeply thankful to the faculty members of the K-State Department of Mathematics for their unwavering support and valuable contributions, which have greatly enriched my academic journey. I extend profound gratitude to Dr. Victor Turchin and Dr. Paul Arnaud Songhafouo for their support and invaluable guidance.

I extend my heartfelt appreciation to my mentor and collaborator, Dr. Olena Burkovska, for her invaluable guidance and support since meeting her in 2023. I am also thankful to the members of Mathematics in Computation (MIC) at the Oak Ridge National Laboratory (ORNL) for their support, and words of encouragement. I am honored and privileged to have had the chance to meet with such exceptional individuals.

Lastly, I am immensely grateful to my family and friends. Their unwavering love and support have been the cornerstone of my success and the driving force behind my perseverance. Their constant encouragement, patience, and belief in me have been a source of strength, and I am forever grateful for their sacrifices.

Chapter 1

Introduction

Nonlocal models are continuum models that involve nonlocal interactions. These models capture complex phenomena, such as fractures, discontinuities, and long-range interactions in materials [3]. Nonlocal models have applications across various fields, including materials science [4], engineering [5], financial markets [6], and mechanobiology [7], among others. Peridynamics is a nonlocal theory for continuum mechanics, which is oriented towards modeling problems involving discontinuities and deformation in complex materials. Particles interact through nonlocal forces within a fixed finite distance, and evolution is described by an integro-differential equation whose solution is in general integrable with respect to spatial variable with no additional regularity [3].

A nonlocal Laplace operator is defined by

$$\mathcal{L}^{\delta,\beta}u(x) = \int_{\mathbb{R}^n} \gamma(x,y)(u(y)-u(x))dy, \;\; x \in \mathbb{R}^n \tag{1.1}$$

for a symmetric kernel $\gamma(x,y) = \gamma(y,x)$ with compact support. In peridynamics, the compact set is the ball of radius δ centered at x. In this dissertation, we focus on radially symmetric kernels with compact support of the form

$$\gamma(x,y) = c^{\delta,\beta}\frac{1}{\|y-x\|^{\beta}}\chi_{B_\delta(x)}(y),$$

where $\chi_{B_\delta(x)}$ is the indicator function of the ball of radius $\delta > 0$ centered at x, the exponent satisfies $\beta < n+2$, and the scaling constant $c^{\delta,\beta}$ is given by

$$c^{\delta,\beta} = \frac{2(n+2-\beta)\Gamma(\frac{n}{2}+1)}{\pi^{\frac{n}{2}}\delta^{n+2-\beta}}.$$

Nonlocal integral operators with compact support of the form (1.1) have their roots in peridynamics [8, 9] and have been introduced in nonlocal vector calculus [10]. These operators have been used in different applied settings such as dynamic brittle fracture [5], image processing [11], tumor growth [7], material failure and damage [4], among others. There have been several mathematical analysis and computational studies involving nonlocal Laplace operators and peridynamic operators, see for example [1, 12–21]. On the mathematical side, the work in [17] introduces the Fourier multipliers for nonlocal Laplace operators, studies the asymptotic behavior of these multipliers, and then applies the asymptotic analysis in the periodic setting to prove regularity results for the nonlocal Poisson equation. In this dissertation, we apply this Fourier multipliers approach to study the regularity of solutions to the nonlocal diffusion equation given by

$$\begin{cases} u_t(x,t) = \mathcal{L}^{\delta,\beta}u(x,t) + b(x), \ x \in T^n, \ t > 0, \\ u(x,0) = f(x), \end{cases} \tag{1.2}$$

over the space of periodic distributions $H^s(T^n)$, with $s \in \mathbb{R}$. Here T^n denotes the periodic torus in $\mathbb{R}^n$ and $\mathcal{L}^{\delta,\beta}$ is a nonlocal Laplace operator defined in (1.1).

On the computational side, we propose an efficient and accurate spectral method for solving nonlocal equations on bounded domains. Spectral methods are accurate and efficient for solving nonlocal equations because they transform integrals in the nonlocal formulation into multiplication in Fourier space. For example, the application of the operator $\mathcal{L}^{\delta,\beta}$ on a function u results in multiplication in Fourier space, and this runs at a computational cost of $\mathcal{O}(N\log N)$ for an N-point discretization grid. For comparison of the efficiency and accuracy of spectral methods versus standard numerical methods such as finite differences, see [1]. Some spectral methods for nonlocal equations have been developed in [1, 22–26]. The work in [23] introduces a boundary-adapted spectral method for peridynamic diffusion problems with arbitrary boundary conditions. A spectral method for nonlocal equations on periodic domains has also been developed in [1], which has been shown to be highly accurate. One difficulty that arises in adapting the spectral method developed in [1] to solve nonlocal equations on bounded domains is that the solutions are in general nonperiodic, therefore exhibiting the Gibbs phenomenon as the Fourier coefficients of the solution decay slowly. One way around this is to use Fourier Continuation. The idea behind Fourier Continuation is to reduce the impact of slowly decaying Fourier coefficients of a smooth but nonperiodic function on a given domain by constructing a smooth periodic extension of the function over a larger domain.

Our approach builds on the Fourier spectral method developed in [1] for periodic domains and incorporate the two-dimensional Fourier Continuation (2D-FC) algorithm from [2] to solve two-dimensional nonlocal equations on bounded domains. We also use this approach to perform numerical experiments aimed at exploring the regularity of solutions for nonlocal equations, with particular focus on discontinuities. For integrable kernels, numerical simulations indicate that discontinuities may develop in the solution. In contrast, for singular kernels with $\beta > n+1 = 3$, the solution appear to remain continuous in the interior of the domain, and no discontinuities are observed.

1.1 Fourier multipliers

In this section, we give a summary of the Fourier multipliers' results introduced in [17], which are relevant to the work presented in Chapters 2 and 3. The Fourier multipliers $m^{\delta,\beta}$ of the nonlocal operator $\mathcal{L}^{\delta,\beta}$ are defined through Fourier transform by

$$\widehat{\mathcal{L}^{\delta,\beta} u} = m^{\delta,\beta} \hat{u}, \tag{1.3}$$

where $m^{\delta,\beta}(\nu)$ is given by the integral representation

$$m^{\delta,\beta}(\nu) = c^{\delta,\beta} \int_{B_\delta(0)} \frac{\cos(\nu \cdot z) - 1}{\|z\|^\beta} dz, \tag{1.4}$$

for $\beta < n + 2$. These multipliers are used to obtain the eigenvalues of the nonlocal operator $\mathcal{L}^{\delta,\beta}$ in the case of periodic domains by evaluating them on a lattice of points (see Section 4.1 of [17]). The following theorem gives a representation of these multipliers using the hypergeometric function, ${}_2F_3$, which is defined by

$${}_2F_3(a_1, a_2; b_1, b_2, b_3, z) := \sum_{k=0}^{\infty} \frac{(a_1)_k (a_2)_k}{(b_1)_k (b_2)_k (b_3)_k} \frac{z^k}{k!},$$

where $(a)_k = a(a+1)(a+2)\cdots(a+k-1)$ is the rising factorial.

Theorem 1.1. *Let $n \geq 1$, $\delta > 0$, and $\beta < n + 2$. Then the Fourier multipliers can be written as*

$$m^{\delta,\beta}(\nu) = -\|\nu\|^2 \ {}_2F_3\left(1, \frac{n+2-\beta}{2}; 2, \frac{n+2}{2}, \frac{n+4-\beta}{2}; -\frac{1}{4}\|\nu\|^2\delta^2\right). \tag{1.5}$$

The hypergeometric function ${}_2F_3$ on the right hand side is well-defined for any $\beta \neq n+4, n+6, \cdots$, hence, using (1.5), the definition of the multipliers is extended to the case when $\beta \geq n+2$ with $\beta \neq n+4, n+6, \cdots$. Consequently, the operator $\mathcal{L}^{\delta,\beta}$ is extended to these larger values of β using the Fourier transform. In particular, for the case when $\beta = n + 2$, and since $m^{\delta,n+2}(\nu)$ is equal to $-\|\nu\|^2$, the extended operator $\mathcal{L}^{\delta,\beta}$ coincides with the classical Laplace operator Δ. For the case, $n + 2 < \beta < n + 4$, the extended operator $\mathcal{L}^{\delta,\beta}$ corresponds to a *nonlocal super-diffusion operator* [1].

The representation (1.5) is used to provide the asymptotic behavior of $m^{\delta,\beta}(\nu)$ for large $\|\nu\|$. This is given by the following result [17].

Theorem 1.2. *Let $n \geq 1$, $\delta > 0$ and $\beta \notin \{n+2, n+4, n+6, \ldots\}$. Then, as $\|\nu\| \to \infty$,*

$$m^{\delta,\beta}(\nu) \sim \begin{cases} -\frac{2n(n+2-\beta)}{\delta^2(n-\beta)} + 2\left(\frac{2}{\delta}\right)^{n+2-\beta} \frac{\Gamma\left(\frac{n+4-\beta}{2}\right)\Gamma\left(\frac{n+2}{2}\right)}{(n-\beta)\Gamma\left(\frac{\beta}{2}\right)} \|\nu\|^{\beta-n}, & \text{if } \beta \neq n, \\ -\frac{2n}{\delta^2}\left(2\log\|\nu\| + \log\left(\frac{\delta^2}{4}\right) + \gamma - \psi\left(\frac{n}{2}\right)\right), & \text{if } \beta = n, \end{cases} \tag{1.6}$$

where γ is Euler's constant and ψ is the digamma function.

Chapter 2

Regularity of solutions for nonlocal diffusion equations with initial data

In this chapter, we apply the Fourier multipliers approach developed in [17] to study the regularity of solutions to the nonlocal diffusion equation with initial data given by

$$\begin{cases} u_t(x,t) = \mathcal{L}^{\delta,\beta} u(x,t), \ x \in T^n, \ t > 0, \\ u(x,0) = f(x). \end{cases} \tag{2.1}$$

To study the existence, uniqueness, and regularity of solutions to nonlocal diffusion equations over the space of periodic distributions, we consider the identification $U(t) = u(\cdot, t)$, with $U : [0, \infty) \to H^s(T^n)$.

2.1 Eigenvalues on periodic domains

Let $\mathcal{L}^{\delta,\beta}$ be defined on the periodic torus

$$T^n = \prod_{i=1}^{n} [0, r_i], \ r_i > 0, \ i = 1, 2, \cdots, n.$$

Define

$$\nu_k = \left(\frac{2\pi k_1}{r_1}, \frac{2\pi k_2}{r_2}, \ldots, \frac{2\pi k_n}{r_n}\right),$$

for any $k \in \mathbb{Z}^n$. Let $\phi_k(x) = e^{i\nu_k \cdot x}$. Then,

$$\mathcal{L}^{\delta,\beta}\phi_k(x) = m^{\delta,\beta}(\nu_k)\phi_k(x), \tag{2.2}$$

which shows that ϕ_k is an eigenfunction of $\mathcal{L}^{\delta,\beta}$ with eigenvalues $m^{\delta,\beta}(\nu_k)$. We will often use $m(\nu)$ to denote $m^{\delta,\beta}(\nu)$ to simplify the notation.

Consider the nonlocal diffusion equation defined in (2.1). For $s \in \mathbb{R}$, let $H^s(T^n)$ be the space of periodic distributions h on T^n such that

$$\|h\|^2_{H^s(T^n)} := \sum_{k\in\mathbb{Z}^n} (1 + \|k\|^2)^s |\hat{h}_k|^2 < \infty.$$

2.2 Distributional solutions for nonlocal diffusion equation

Let $f \in H^s(T^n)$ and define $U, V : [0, \infty) \to H^q(T^n)$ for some $q \in \mathbb{R}$, by

$$U(t) = \sum_k \hat{f}_k e^{m(\nu_k)t} e^{i\nu_k\cdot x}, \tag{2.3}$$

$$V(t) = \sum_k \hat{f}_k m(\nu_k) e^{m(\nu_k)t} e^{i\nu_k\cdot x}. \tag{2.4}$$

Observe that for any $t \geq 0$, $U(t)$ and $V(t)$ are well-defined periodic distributions, since $e^{m(\nu_k)t}$ and $m(\nu_k)e^{m(\nu_k)t}$ are both bounded functions in k.

Theorem 2.1. *Let $n \geq 1$, $\delta > 0$ and $\beta < n+4$. Let ε_1 and ε_2 be such that $0 < \varepsilon_1 < \varepsilon_2 < 1$. Assume that $f \in H^s(T^n)$ for some $s \in \mathbb{R}$. Then for any fixed $t > 0$, $U(t) \in H^p(T^n)$ and*

$V(t) \in H^r(T^n)$, *where*

$$p \;=\; \begin{cases} s, \;\; \textit{if } \beta < n, \\ s + \dfrac{4nt}{\delta^2}(1-\varepsilon_1), \;\; \textit{if } \beta = n, \\ \infty, \;\; \textit{if } \beta > n, \end{cases} \qquad r = \begin{cases} s, \;\; \textit{if } \beta < n, \\ s + \dfrac{4nt}{\delta^2}(1-\varepsilon_2), \;\; \textit{if } \beta = n, \\ \infty, \;\; \textit{if } \beta > n, \end{cases} \tag{2.5}$$

with $H^\infty(T^n) := \bigcap_{s \in \mathbb{R}} H^s(T^n)$.

Proof. We observe that

$$\sum_{0 \neq k \in \mathbb{Z}^n} (1 + \|k\|^2)^p |\hat{U}_k|^2 = \sum_{0 \neq k \in \mathbb{Z}^n} (1 + \|k\|^2)^{p-s} (1 + \|k\|^2)^s |\hat{f}_k e^{m(\nu_k)t}|^2.$$

Since $f \in H^s(T^n)$, then the result that $U(t) \in H^p(T^n)$ follows by showing that

$$(1 + \|k\|^2)^{p-s} e^{2m(\nu_k)t}$$

is bounded for $k \neq 0$. To see this, we consider three cases. For the case $\beta < n$, then $p - s = 0$ and

$$e^{2m(\nu_k)t}(1 + \|k\|^2)^{p-s} = e^{2m(\nu_k)t},$$

which is bounded since $m(\nu_k) \leq 0$.

For the case when $n < \beta < n + 4$, let $q \in \mathbb{R}$ be arbitrary. Then,

$$(1 + \|k\|^2)^{q-s} e^{2m(\nu_k)t} = \frac{(1 + \|k\|^2)^{q-s}}{e^{2t|m(\nu_k)|}},$$

which vanishes as $\|k\| \to \infty$, and hence boundedness follows. Thus, $U(t) \in H^q(T^n)$ for all q and therefore,

$$U(t) \in \bigcap_{q \in \mathbb{R}} H^q(T^n) = H^\infty(T^n).$$

For the case when $\beta = n$, then $p - s = \frac{4nt}{\delta^2}(1-\varepsilon_1)$. From Theorem 1.2, we have

$$m(\nu_k) \sim -\frac{4n}{\delta^2}\log\|\nu_k\|,$$

which implies that

$$\lim_{\|\nu_k\|\to\infty} \frac{m(\nu_k)}{-\frac{4n}{\delta^2}\log\|\nu_k\|} = 1. \tag{2.6}$$

Thus, for any $\varepsilon_1 > 0$, there exists $N \in \mathbb{N}$ such that

$$-\frac{4n}{\delta^2}(1+\varepsilon_1)\log\|\nu_k\| \le m(\nu_k) \le -\frac{4n}{\delta^2}(1-\varepsilon_1)\log\|\nu_k\|, \tag{2.7}$$

for all $\|\nu_k\| \ge N$. Therefore,

$$e^{2m(\nu_k)t} \quad \le \quad e^{-\frac{8nt}{\delta^2}(1-\varepsilon_1)\log\|\nu_k\|} = \|\nu_k\|^{-\frac{8nt}{\delta^2}(1-\varepsilon_1)}. \tag{2.8}$$

Since there exists $A > 0$ such that $A\|k\| \le \|\nu_k\|$, then

$$(1+\|k\|^2)^{p-s}e^{2m(\nu_k)t} \quad \le \quad \frac{(1+\|k\|^2)^{\frac{4nt}{\delta^2}(1-\varepsilon_1)}}{\|\nu_k\|^{\frac{8nt}{\delta^2}(1-\varepsilon_1)}} \le \frac{(1+\|k\|^2)^{\frac{4nt}{\delta^2}(1-\varepsilon_1)}}{(A\|k\|)^{\frac{8nt}{\delta^2}(1-\varepsilon_1)}},$$

which is bounded.

Similarly, to show that $V(t) \in H^r(T^n)$, we show that

$$(1+\|k\|^2)^{r-s}m(\nu_k)^2e^{2m(\nu_k)t}$$

is bounded for $k \ne 0$. For the case when $\beta < n$, then $r - s = 0$ and there exists a constant $C > 0$ such that $|m(\nu_k)| \le C$. Thus,

$$(1+\|k\|^2)^{r-s}m(\nu_k)^2e^{2m(\nu_k)t} = m(\nu_k)^2e^{2m(\nu_k)t}$$

is bounded. For the case when $n < \beta < n+4$, then for an arbitrary $q' \in \mathbb{R}$, we have

$$(1+\|k\|^2)^{q'-s} m(\nu_k)^2 e^{2m(\nu_k)t} = \frac{m(\nu_k)^2(1+\|k\|^2)^{q'-s}}{e^{2t|m(\nu_k)|}},$$

which vanishes as $\|k\| \to \infty$, and therefore boundedness follows. Thus, $V(t) \in H^{q'}(T^n)$ for all $q' \in \mathbb{R}$ and hence,

$$V(t) \in \bigcap_{q' \in \mathbb{R}} H^{q'}(T^n) = H^\infty(T^n).$$

When $\beta = n$, then $r - s = \frac{4nt}{\delta^2}(1-\varepsilon_2)$. From (2.7),

$$|m(\nu_k)|^2 \leq \left(\frac{4n}{\delta^2}(1+\varepsilon_1)\right)^2 (\log\|\nu_k\|)^2. \tag{2.9}$$

In addition, there exists $N_2 \in \mathbb{N}$ such that

$$\log(\|\nu_k\|) \leq \|\nu_k\|^{\frac{4nt}{\delta^2}(\varepsilon_2-\varepsilon_1)}, \tag{2.10}$$

for all $\|\nu_k\| > N_2$. Moreover, there exists $B > 0$ such that $\|\nu_k\| \leq B\|k\|$. Hence, by using (2.8), (2.9), and (2.10), we obtain

$$\begin{aligned} (1+\|k\|^2)^{r-s}|m(\nu_k)|^2 e^{2m(\nu_k)t} &\leq \frac{(1+\|k\|^2)^{\frac{4nt}{\delta^2}(1-\varepsilon_2)}\left(\frac{4n}{\delta^2}(1+\varepsilon_1)\right)^2 (B^2\|k\|^2)^{\frac{4nt}{\delta^2}(\varepsilon_2-\varepsilon_1)}}{(A\|k\|)^{\frac{8nt}{\delta^2}(1-\varepsilon_1)}} \\ &= M\frac{(1+\|k\|^2)^{\frac{4nt}{\delta^2}(1-\varepsilon_2)}}{\|k\|^{\frac{8nt}{\delta^2}(1-\varepsilon_2)}}, \end{aligned}$$

where

$$M = \frac{\left(\frac{4n}{\delta^2}(1+\varepsilon_1)\right)^2 B^{\frac{8nt}{\delta^2}(\varepsilon_2-\varepsilon_1)}}{A^{\frac{8nt}{\delta^2}(1-\varepsilon_1)}}.$$

This shows boundedness and therefore completing the proof. □

For any $J \in H^s(T^n),\ s \in \mathbb{R}$, define

$$\mathcal{L}^{\delta,\beta} J = \sum_{k \in \mathbb{Z}^n} m(\nu_k)\hat{J}_k e^{i\nu_k \cdot x}. \tag{2.11}$$

Lemma 2.1. *Let U and V be as defined in (2.3) and (2.4) respectively, then $\mathcal{L}^{\delta,\beta}U(t) = V(t)$.*

Proof. By (2.11), we have

$$\begin{aligned}
\mathcal{L}^{\delta,\beta}U(t) &= \sum_{k\in\mathbb{Z}^n} m(\nu_k)\hat{U}_k(t)e^{i\nu_k\cdot x} \\
&= \sum_{k\in\mathbb{Z}^n} m(\nu_k)\hat{f}_k e^{m(\nu_k)t}e^{i\nu_k\cdot x} \\
&= V(t).
\end{aligned}$$

□

Proposition 2.1. *Let $N \in \mathbb{N}\cup\{0\}$ and define*

$$\begin{aligned}
U^{(N)}(t) &= \sum_k \hat{f}_k m(\nu_k)^N e^{m(\nu_k)t}e^{i\nu_k\cdot x}, \\
V^{(N)}(t) &= \sum_k \hat{f}_k m(\nu_k)^{N+1} e^{m(\nu_k)t}e^{i\nu_k\cdot x}.
\end{aligned}$$

Then $\frac{d}{dt}U^{(N)}(t) = V^{(N)}(t)$, for all $t \in (0,\infty)$. Equivalently,

$$\frac{d^N}{dt^N}U(t) = \sum_k \hat{f}_k m(\nu_k)^{N+1} e^{m(\nu_k)t}e^{i\nu_k\cdot x},$$

where the differentiation here is in the sense of Gateaux differentiation.

Remark 2.1. *We note that $U^{(0)}(t) = U(t)$ and $V^{(0)}(t) = V(t)$. In addition, similar to the argument in Theorem 2.1, for any $t \geq 0$, both $U^{(N)}(t)$ and $V^{(N)}(t)$ are in $H^s(T^n)$ when $\beta \leq n$ and both are in $H^\infty(T^n)$ when $n < \beta < n+4$.*

Proof. Let $t > 0$, we show that $\frac{d}{dt}U^{(N)}(t) = V^{(N)}(t)$, where the differentiation is in the Gateaux sense, which is given by

$$\lim_{h\to 0}\left\|\frac{1}{h}\left[U^{(N)}(t+h) - U^{(N)}(t)\right] - V^{(N)}(t)\right\|^2_{H^q(T^n)} = 0,$$

where $q = s$ when $\beta \leq n$ and q is arbitrary when $n < \beta < n+4$. Equivalently, we show that

$$\lim_{h\to 0} \sum_{k\in\mathbb{Z}^n} (1+\|k\|^2)^q |\hat{f}_k|^2 m(\nu_k)^{2N} \left[\frac{1}{h}\left(e^{m(\nu_k)h}-1\right)e^{m(\nu_k)t} - m(\nu_k)e^{m(\nu_k)t}\right]^2 = 0. \tag{2.12}$$

This result follows from passing the limit inside the sum, which we justify next by the dominated convergence theorem.

When $\beta < n$, then $q = s$ and there exists a constant $C_1 > 0$ such that $|m(\nu_k)| < C_1$. Moreover, there exists $C_2 > 0$ such that

$$\left|\frac{e^{m(\nu_k)h}-1}{h}\right| < C_2, \tag{2.13}$$

for all k, and for sufficiently small h. Combining this with the fact that $f \in H^s(T^n)$, it follows that the summand in the left hand side of (2.12) is uniformly bounded.

For the cases $\beta > n$ and $\beta = n$, we note that the summand in (2.12) can be written as

$$(1+\|k\|^2)^s |f_k|^2 \left(\frac{e^{m(\nu_k)h}-1-m(\nu_k)h}{h}\right)^2 e^{2m(\nu_k)t} m(\nu_k)^{2N} (1+\|k\|^2)^{q-s}.$$

Since $f \in H^s(T^n)$, then it is left to show that

$$\left(\frac{e^{m(\nu_k)h}-1-m(\nu_k)h}{h}\right)^2 e^{2m(\nu_k)t} m(\nu_k)^{2N} (1+\|k\|^2)^{q-s} \tag{2.14}$$

is uniformly bounded. By Taylor's Theorem,

$$\left(\frac{e^{m(\nu_k)h}-1-m(\nu_k)h}{h}\right) \leq \frac{m(\nu_k)^2}{2}, \tag{2.15}$$

for all $h \in (0,1)$. Therefore,

$$\left(\frac{e^{m(\nu_k)h}-1-m(\nu_k)h}{h}\right)^2 e^{2m(\nu_k)t} m(\nu_k)^{2N} (1+\|k\|^2)^{q-s} \leq \frac{1}{4}(1+\|k\|^2)^{q-s} m(\nu_k)^{2N+4} e^{2m(\nu_k)t}.$$

For $\beta = n$, then $q - s = 0$ and since $m(\nu_k) \to -\infty$ as $\|k\| \to \infty$, then

$$\frac{1}{4} m(\nu_k)^{2N+4} e^{2m(\nu_k)t} \to 0$$

as $\|k\| \to \infty$, showing that (2.14) is uniformly bounded.

For $\beta > n$, then by using Theorem 1.2, we have that

$$\frac{1}{4}(1 + \|k\|^2)^{q-s} m(\nu_k)^{2N+4} e^{2m(\nu_k)t} = \frac{(1 + \|k\|^2)^{q-s} m(\nu_k)^{2N+4}}{4e^{2|m(\nu_k)|t}} \to 0$$

as $\|k\| \to \infty$, showing that (2.14) is uniformly bounded and therefore completing proof. $\square$

The following theorem summarizes the results in this section.

Theorem 2.2. *Let $f \in H^s(T^n)$, $\beta < n + 4$, and $s \in \mathbb{R}$. Then, there exists a unique solution $U(t)$ to the nonlocal diffusion equation*

$$\begin{cases} \dfrac{dU}{dt} = \mathcal{L}^{\delta,\beta} U(t), \\ U(0) = f. \end{cases} \tag{2.16}$$

Moreover, $U \in C^\infty((0, \infty); H^p(T^n))$, where p is as defined in (2.5).

Remark 2.2. *The time regularity in Theorem 2.2 is in the sense of Gateaux differentiation.*

Proof. The existence follows from Lemma 2.1 and Proposition 2.1 by taking $N = 0$. For the uniqueness, let $Q(t)$ be another solution of (2.16). We define $W(t) = U(t) - Q(t)$. Then, $W(t)$ satisfies

$$\begin{cases} \dfrac{dW}{dt} = \mathcal{L}^{\delta,\beta} W, \\ W(0) = 0. \end{cases}$$

Represent $W(t)$ by its Fourier series

$$W(t) = \sum_{k \in \mathbb{Z}^n} \hat{W}_k(t) e^{i\nu_k \cdot x}.$$

Lemma 2.1 implies that

$$\mathcal{L}^{\delta,\beta}W(t) = \sum_{k\in\mathbb{Z}^n} m(\nu_k)\hat{W}_k(t)e^{i\nu_k\cdot x},$$

and

$$\frac{dW}{dt} = \sum_{k\in\mathbb{Z}^n} \frac{d\hat{W}_k}{dt}(t)e^{i\nu_k\cdot x}.$$

From (2.16) and the uniqueness of Fourier coefficients, we have that

$$\frac{d\hat{W}_k}{dt}(t) = m(\nu_k)\hat{W}_k(t),$$

for all k. This implies that $\hat{W}_k(t) = Ae^{m(\nu_k)t}$, where A is a constant. Since $\hat{W}_k(0) = 0$, then $\hat{W}_k(t) = 0$, for all k which implies that $W(t) = 0$. Therefore, $U(t) = Q(t)$. The spatial regularity follows from Theorem 2.1. $\square$

2.3 Regular functions as solutions of the nonlocal diffusion equation

In this section, we focus on functions f that satisfy $\sum_{k\in\mathbb{Z}^n} |\hat{f}_k| < \infty$. The following theorem gives a class of functions that satisfy this condition, see [27].

Theorem 2.3. *Let s be a nonnegative integer and let $0 \leq \alpha < 1$. Assume that f is a function defined on T^n all of whose partial derivatives of order s lie in the space of Holder continuous functions of order α. Suppose that $s+\alpha > n/2$. Then f has an absolutely convergent Fourier series.*

Next, we provide results on the temporal regularity of the nonlocal diffusion equation.

Proposition 2.2. *Let $f \in H^s(T^n)$ such that $\sum_{k\in\mathbb{Z}^n} |\hat{f}_k| < \infty$ and let $\beta < n + 4$. Then,*

$$u(x,\cdot) \in C^\infty((0,\infty)),\ \forall x \in T^n.$$

Proof. We use the Leibniz integral rule for the counting measure to differentiate under the summation. Let $g_k(t) = \hat{f}_k e^{m(\nu_k)t} e^{i\nu_k \cdot x}$ and consider

$$\begin{aligned}\sum_{k\in\mathbb{Z}^n} |g_k(t)| &= \sum_{k\in\mathbb{Z}^n} |\hat{f}_k e^{m(\nu_k)t} e^{i\nu_k\cdot x}| \\ &= \sum_{k\in\mathbb{Z}^n} |\hat{f}_k| e^{m(\nu_k)t} \\ &\leq \sum_{k\in\mathbb{Z}^n} |\hat{f}_k|.\end{aligned}$$

Since $\sum\limits_{k\in\mathbb{Z}^n} |\hat{f}_k| < \infty$, then $g_k(t)$ is summable for any fixed t. Moreover,

$$\frac{dg_k}{dt} = \hat{f}_k m(\nu_k) e^{m(\nu_k)t} e^{i\nu_k\cdot x},$$

is continuous for all k. Now fix $t > 0$, then there exist τ such that $0 < \tau < t$. We define $\theta_k := |\hat{f}_k||m(\nu_k)|e^{m(\nu_k)\tau}$. When $\beta < n$, then there exists $C > 0$ such that $|m(\nu_k)| \leq C$. Thus

$$\theta_k = |\hat{f}_k||m(\nu_k)|e^{m(\nu_k)\tau} \leq C|\hat{f}_k|,$$

showing that θ_k is summable. When $\beta \geq n$, then $e^{m(\nu_k)\tau} \to 0$ as $\|k\| \to \infty$. Thus $|m(\nu_k)|e^{m(\nu_k)\tau} \leq 1$ for sufficiently large $\|k\|$. Hence $\theta_k \leq |\hat{f}_k|$, showing that θ_k is summable. Moreover

$$\begin{aligned}\left|\frac{dg_k}{dt}\right| &= |\hat{f}_k||m(\nu_k)|e^{m(\nu_k)t} \\ &\leq |\hat{f}_k||m(\nu_k)|e^{m(\nu_k)\tau} \\ &= \theta_k.\end{aligned}$$

Therefore, we can differentiate under the summation,

$$\begin{aligned}
\frac{\partial u(x,t)}{\partial t} &= \frac{d}{dt}\sum_{k\in\mathbb{Z}^n} g_k(t) \\
&= \sum_{k\in\mathbb{Z}^n} \frac{dg_k}{dt} \\
&= \sum_{k\in\mathbb{Z}^n} \hat{f}_k m(\nu_k) e^{m(\nu_k)t} e^{i\nu_k\cdot x}.
\end{aligned}$$

For higher derivatives, we observe that

$$\frac{d^N g_k}{dt^N} = \hat{f}_k |m(\nu_k)|^N e^{m(\nu_k)t} e^{i\nu_k\cdot x}.$$

Define $\psi_k = |\hat{f}_k||m(\nu_k)|^N e^{m(\nu_k)\tau}$. Then ψ_k is summable by following similar arguments as above. Furthermore,

$$\begin{aligned}
\left|\frac{d^N g_k}{dt^N}\right| &= |\hat{f}_k||m(\nu_k)|^N e^{m(\nu_k)t} \\
&\leq |\hat{f}_k||m(\nu_k)|^N e^{m(\nu_k)\tau} \\
&= \psi_k.
\end{aligned}$$

This implies that $u(x,\cdot)$ is N-times continuously differentiable and

$$\begin{aligned}
\frac{\partial^N u(x,t)}{\partial t^N} &= \frac{d^N}{dt^N}\sum_{k\in\mathbb{Z}^n} g_k(t) \\
&= \sum_{k\in\mathbb{Z}^n} \frac{d^N g_k}{dt^N} \\
&= \sum_{k\in\mathbb{Z}^n} \hat{f}_k |m(\nu_k)|^N e^{m(\nu_k)t} e^{i\nu_k\cdot x}.
\end{aligned}$$

Since N is arbitrary, it follows that $u(x,\cdot) \in C^\infty((0,\infty))$. □

From Theorem 2.1 and Proposition 2.2 we obtain the following regularity result.

Theorem 2.4. *Let $n \geq 1$, $\delta > 0$, $\varepsilon > 0$ and $\beta < n+4$. Assume that $f \in H^s(T^n)$ and its*

Fourier coefficients are summable. Then,

1. $u \in C^\infty((0,\infty); H^s(T^n))$ *for* $\beta < n$,

2. $u \in C^\infty\left((0,\infty); H^{s+\frac{4nt}{\delta^2}(1-\varepsilon)}(T^n)\right)$ *for* $\beta = n$,

3. $u \in C^\infty((0,\infty); H^\infty(T^n))$ *for* $\beta > n$.

The following lemma will be used to prove Theorem 2.5 on the convergence of solutions of the nonlocal diffusion equation as $\delta \to 0^+$.

Lemma 2.2. *Let* $n < \beta < n+2$ *and* $\delta \leq 1$. *Then, there exist* $c_1 > 0$ *and* $c_2 > 0$ *such that*

$$m^{\delta,\beta}(\nu) \leq \max\{-c_1\|\nu\|^{\beta-n}, -c_2\|\nu\|^2\}, \ \forall \nu \in \mathbb{R}^n$$

Proof. From Theorem 1.2, we have

$$m^{1,\beta}(\nu) \sim c\|\nu\|^{\beta-n},$$

where

$$c = (2)2^{n+2-\beta}\frac{\Gamma\left(\frac{n+4-\beta}{2}\right)\Gamma\left(\frac{n+2}{2}\right)}{(\beta-n)\Gamma\left(\frac{\beta}{2}\right)} > 0.$$

This is equivalent to

$$\lim_{\|\nu\|\to\infty}\frac{m^{1,\beta}(\nu)}{-\|\nu\|^{\beta-n}} = c,$$

which implies that there is $c_1 > 0$ and $N > 0$ such that for all $\|\nu\| > N$

$$m^{1,\beta}(\nu) \leq -c_1\|\nu\|^{\beta-n}. \tag{2.17}$$

On the other hand, from [17], we have

$$\lim_{\|\nu\|\to 0}\frac{m^{1,\beta}(\nu)}{-\|\nu\|^{\beta-n}} = 1.$$

Thus, there exists $c_2 > 0$ such that for all $\|\nu\| < N$,

$$m^{1,\beta}(\nu) \leq -c_2\|\nu\|^2. \tag{2.18}$$

Combining (2.17) and (2.18), we have

$$m^{1,\beta}(\nu) \leq \max\{-c_1\|\nu\|^{\beta-n}, -c_2\|\nu\|^2\}, \tag{2.19}$$

for all $\nu \in \mathbb{R}^n$. Using (2.19) and the fact that $m^{\delta,\beta}(\nu) = \frac{1}{\delta^2}m^{1,\beta}(\delta\nu)$, which follows from (1.5), we obtain

$$\begin{aligned} m^{\delta,\beta}(\nu) = \frac{1}{\delta^2}m^{1,\beta}(\delta\nu) &\leq \frac{1}{\delta^2}\max\{-c_1\|\delta\nu\|^{\beta-n}, -c_2\|\delta\nu\|^2\} \\ &= \max\{-c_1\|\nu\|^{\beta-n}\delta^{\beta-(n+2)}, -c_2\|\nu\|^2\}. \end{aligned}$$

Since $\delta \leq 1$, then $-\delta^{\beta-(n+2)} \leq -1$ and hence

$$m^{\delta,\beta}(\nu) \leq \max\{-c_1\|\nu\|^{\beta-n}, -c_2\|\nu\|^2\}.$$

$\square$

Convergence of solutions of the nonlocal diffusion equation (2.1) to the solution of the corresponding classical diffusion equation is given next in Theorem 2.5 and Theorem 2.6.

Theorem 2.5. *Let $n \geq 1, s \in \mathbb{R}$ and let $f \in H^s(T^n)$. Suppose u is the solution of the classical diffusion equation $u_t = \Delta u$ with initial condition $u|_{t=0} = f$. For any $\delta > 0$, let $u^{\delta,\beta}$ be the solution of the nonlocal diffusion equation in (2.1). Then, for $t > 0$ and $\beta \leq n$,*

$$\lim_{\delta \to 0^+} u^{\delta,\beta}(\cdot, t) = u(\cdot, t), \quad \textit{in } H^s(T^n),$$

and for $n < \beta \leq n+2$,

$$\lim_{\delta \to 0^+} u^{\delta,\beta}(\cdot, t) = u(\cdot, t), \quad \textit{in } H^{\infty}(T^n).$$

Proof. The Fourier coefficients satisfy $\hat{u}_k^{\delta,\beta} = \hat{f}_k e^{m(\nu_k)t}$ and $\hat{u}_k = \hat{f}_k e^{-\|\nu_k\|^2 t}$. When $\beta \leq n$, then

$$\begin{aligned} \|u^{\delta,\beta}(\cdot,t) - u(\cdot,t)\|^2_{H^s(T^n)} &= \sum_{0 \neq k \in \mathbb{Z}^n} (1+\|k\|^2)^s \ |\hat{u}_k^{\delta,\beta} - \hat{u}_k|^2 \\ &= \sum_{0 \neq k \in \mathbb{Z}^n} (1+\|k\|^2)^s \ |e^{m(\nu_k)t} - e^{-\|\nu_k\|^2 t}|^2 \ |\hat{f}_k|^2. \end{aligned}$$

To pass the limit $\delta \to 0^+$ inside the sum, it is sufficient to show that $|e^{m(\nu_k)t} - e^{-\|\nu_k\|^2 t}|^2$ as a function of k is uniformly bounded. Using (1.4), it is straightforward to see that $m(\nu) \leq 0$ for $\nu \in \mathbb{R}^n$. Thus,

$$\left| e^{m(\nu_k)t} - e^{-\|\nu_k\|^2 t} \right|^2 \leq (e^{m(\nu_k)t} + e^{-\|\nu_k\|^2 t})^2 \leq 4.$$

Since, $\lim_{\delta \to 0^+} m(\nu_k) = -\|\nu_k\|^2$, then

$$\lim_{\delta \to 0^+} u^{\delta,\beta}(\cdot, t) = u(\cdot, t), \quad \text{in } H^s(T^n).$$

For the case $\beta > n$, fix an arbitrary $p \in \mathbb{R}$. Then,

$$\begin{aligned} \|u^{\delta,\beta}(\cdot,t) - u(\cdot,t)\|^2_{H^p(T^n)} &= \sum_{0 \neq k \in \mathbb{Z}^n} (1+\|k\|^2)^p |\hat{u}_k^{\delta,\beta} - \hat{u}_k|^2 \\ &= \sum_{0 \neq k \in \mathbb{Z}^n} (1+\|k\|^2)^s \, (1+\|k\|^2)^{p-s} \ |e^{m(\nu_k)t} - e^{-\|\nu_k\|^2 t}|^2 \ |\hat{f}_k|^2. \end{aligned}$$

Since $(1+\|k\|^2)^s |\hat{f}_k|^2$ is summable, then to pass the limit inside the above sum, we show that the following function in k that is given by

$$(1+\|k\|^2)^{p-s}|e^{m(\nu_k)t}-e^{-\|\nu_k\|^2 t}|^2,$$

is uniformly bounded. First, we rewrite the above expression as

$$(1+\|k\|^2)^{p-s}|e^{m(\nu_k)t}-e^{-\|\nu_k\|^2 t}|^2 \;=\; (1+\|k\|^2)^{p-s}\; e^{2m(\nu_k)t}\left(1-e^{-(m(\nu_k)+\|\nu_k\|^2)t}\right)^2.$$

Then, we observe that

$$\begin{aligned} m^{\delta,\beta}(\nu_k)+\|\nu_k\|^2 &= -\|\nu_k\|^2\;{}_2F_3\left(1,\frac{n+2-\beta}{2};2,\frac{n+2}{2},\frac{n+4-\beta}{2};-\frac{1}{4}\|\nu_k\|^2\delta^2\right)+\|\nu_k\|^2 \\ &= \|\nu_k\|^2\left(1-{}_2F_3\left(1,\frac{n+2-\beta}{2};2,\frac{n+2}{2},\frac{n+4-\beta}{2};-\frac{1}{4}\|\nu_k\|^2\delta^2\right)\right). \end{aligned}$$

Since ${}_2F_3\left(1,\frac{n+2-\beta}{2};2,\frac{n+2}{2},\frac{n+4-\beta}{2};x\right)\leq 1$ for all $x\leq 0$, then $m^{\delta,\beta}+\|\nu_k\|^2\geq 0$. Therefore,

$$1-e^{-(m(\nu_k)+\|\nu_k\|^2)t}<1.$$

Using this fact, we have

$$\begin{aligned} (1+\|k\|^2)^{p-s}\left|e^{m(\nu_k)t}-e^{-\|\nu_k\|^2}\right| &= (1+\|k\|^2)^{p-s}\; e^{2m(\nu_k)t}(1-e^{-(m(\nu_k)+\|\nu_k\|^2t})^2 \\ &< (1+\|k\|^2)^{p-s}\; e^{2m(\nu_k)t}. \end{aligned}$$

Lemma 2.2 implies that there exist $c_1>0$ and $c_2>0$ such that

$$e^{m(\nu_k)t}\leq \max\{e^{-c_1\|\nu_k\|^{\beta-n}\,t},e^{-c_2\|\nu_k\|^2 t}\}.$$

Consequently,

$$(1+\|k\|^2)^{p-s}\; e^{2m(\nu_k)t}\leq \frac{(1+\|k\|^2)^{p-s}}{\min\{\exp(2c_1\|\nu_k\|^{\beta-n}\,t),\exp(2c_2\|\nu_k\|^2 t)\}},$$

which is bounded for sufficiently large k for all $\delta \in [0,1]$. $\square$

Theorem 2.6. *Let $n \geq 1, s \in \mathbb{R}$ and let $f \in H^s(T^n)$. Suppose u is the solution of the classical diffusion equation $u_t = \Delta u$, with $u|_{t=0} = f$, and for any $\beta < n+4$, let $u^{\delta,\beta}$ be the solution of the nonlocal diffusion equation (2.1), then for $t > 0$,*

$$\lim_{\beta \to n+2} u^{\delta,\beta}(\cdot,t) = u(\cdot,t), \ \text{in } H^\infty(T^n).$$

Proof. Let $q \in \mathbb{R}$ be arbitrary. Consider

$$\|u^{\delta,\beta}(\cdot,t) - u(\cdot,t)\|^2_{H^q(T^n)} = \sum_{k\in\mathbb{Z}^n} (1+\|k\|^2)^{q-s} \left| e^{m(\nu_k)t} - e^{-\|\nu_k\|^2 t} \right|^2 (1+\|k\|^2)^s \|\hat{f}_k\|^2.$$

We observe that for β near $n+2$, $m(\nu_k) \to -\infty$ as $\|k\| \to \infty$. Thus, we can pass the limit in β inside the sum above, since $f \in H^s(T^n)$ and the expression

$$(1+\|k\|^2)^{q-s} \left| e^{m(\nu_k)t} - e^{-\|\nu_k\|^2 t} \right|^2,$$

is uniformly bounded. Since $\lim_{\beta\to n+2} m(\nu_k) = -\|\nu_k\|^2$, then the result follows. $\square$

2.4 Propagation of discontinuities for the nonlocal diffusion equation

In this section, we study the propagation of discontinuities for the nonlocal diffusion equation in (2.1). We emphasize that Theorem 2.4 implies that the nonlocal diffusion equation satisfies an instantaneous smoothing effect when the integral kernel is singular with $\beta > n$ and a gradual (over time) smoothing effect for when $\beta = n$. However, for integrable kernels ($\beta < n$), the nonlocal diffusion equation is non-smoothing. In this section, we investigate this latter case further by studying the propagation of discontinuities. To this end, given a discontinuous initial data $f \in L^2(T^n)$. Then, we show that for certain conditions on f and β, discontinuities persist and propagate. In particular, we show that in one-dimension, if f

is piecewise continuous, then the solution u is piecewise continuous and both f and u share the same locations of jumps.

To study the propagation of discontinuities, we look for a decomposition of u, the solution of (2.1), of the form

$$u(x,t) = v(x,t) + g(t)f(x),$$

for some function $v(x,t)$, which is continuous in x and satisfies $v(x,0) = 0$, and some function g satisfying $g(0) = 1$. This would imply that any discontinuity in f will persist to be a discontinuity in u for all $t > 0$. We show that the magnitude of a jump discontinuity decays as t increases.

We observe that v satisfies the following

$$\begin{aligned} v_t &= u_t - g'(t)f(x) \\ &= \mathcal{L}^{\delta,\beta}u - g'(t)f(x) \\ &= \mathcal{L}^{\delta,\beta}v + g(t)\mathcal{L}^{\delta,\beta}f(x) - g'(t)f(x). \end{aligned}$$

Since $\beta < n$, we observe that

$$\mathcal{L}^{\delta,\beta}f(x) = c^{\delta,\beta}\int_{B_\delta(x)} \frac{f(y)-f(x)}{\|y-x\|^\beta}dy = h(x) - \alpha f(x),$$

where

$$h(x) = c^{\delta,\beta}\int_{B_\delta(x)} \frac{f(y)}{\|y-x\|^\beta}dy = \left(\frac{c^{\delta,\beta}}{\|\cdot\|^\beta}\chi_{B_\delta(0)}(\cdot)\right) * f(x), \tag{2.20}$$

and α is a constant given by

$$\alpha = c^{\delta,\beta}\int_{B_\delta(x)} \frac{1}{\|y-x\|^\beta}dy = \frac{2n(n+2-\beta)}{\delta^2(n-\beta)}. \tag{2.21}$$

Therefore,

$$\begin{aligned} v_t &= \mathcal{L}^{\delta,\beta} v + g(t)h(x) - \alpha g(t) f(x) - g'(t) f(x) \\ &= \mathcal{L}^{\delta,\beta} v + g(t)h(x) - f(x)\left(\alpha g(t) - g'(t)\right). \end{aligned}$$

Since $g(t)$ is unknown and we are looking for $v(x,t)$, a continuous function in x which is independent of $f(x)$, we set $\alpha g(t) - g'(t) = 0$. Thus $g(t) = e^{-\alpha t}$ and v solves

$$\begin{cases} v_t = \mathcal{L}^{\delta,\beta} v + e^{-\alpha t} h(x), \ x \in T^n, t > 0, \\ v(x,0) = 0, \end{cases} \tag{2.22}$$

and therefore,

$$u(x,t) = v(x,t) + e^{-\alpha t} f(x). \tag{2.23}$$

Hence,

$$\begin{aligned} \hat{v}_k &= \hat{u}_k - e^{-\alpha t} \hat{f}_k \\ &= \hat{f}_k e^{m(\nu_k)t} - e^{-\alpha t} \hat{f}_k \\ &= \hat{f}_k \left(1 - e^{-(m(\nu_k)+\alpha)t}\right) e^{m(\nu_k)t}. \end{aligned} \tag{2.24}$$

It remains to find conditions on f and β to guarantee the continuity of v. Towards this end, we make use of the following lemma, whose proof is similar to the proof of Theorem 3.2 in [17]. We note that the constant α appears in the asymptotics formula (1.6).

Lemma 2.3. *Let $\nu \in \mathbb{R}^n$ and let $\beta < n$. Suppose α is as defined in (2.21). Then*

$$m(\nu) + \alpha \sim \begin{cases} 4(n+2-\beta)\Gamma\left(\frac{n}{2}+1\right)\delta^2 \dfrac{\Gamma\left(\frac{n}{2}\right)\Gamma\left(\frac{n+2-\beta}{2}\right)}{\Gamma\left(\frac{\beta}{2}\right)} \left(\frac{\delta\|\nu\|}{2}\right)^{\beta-n}, & \text{if } \frac{n-1}{2} < \beta < n, \\ 4(n+2-\beta)\Gamma\left(\frac{n}{2}+1\right)\delta^2 \dfrac{(n-\beta)\Gamma\left(\frac{n}{2}\right)}{4\sqrt{\pi}} \left(\frac{\delta\|\nu\|}{2}\right)^{-\frac{n+1}{2}}, & \text{if } \beta \le \frac{n-1}{2}. \end{cases}$$

In addition, we make use of the following lemma.

Lemma 2.4. *Let α be as defined in (2.21). Then,*

$$\left(1-e^{-(m(\nu_k)+\alpha)t}\right)e^{m(\nu_k)t} \sim \begin{cases} \dfrac{C_1 t e^{-\alpha t}}{\|k\|^{n-\beta}}, & \text{if } \frac{n-1}{2} < \beta < n, \\ \\ \dfrac{C_2 t e^{-\alpha t}}{\|k\|^{\frac{n+1}{2}}}, & \text{if } \beta \leq \frac{n-1}{2}, \end{cases}$$

for some positive constants C_1 and C_2.

Proof. When $\frac{n-1}{2} < \beta < n$, then by using Lemma 2.3 and the definition of ν_k, there exists $C_1 > 0$ such that

$$\lim_{\|k\|\to\infty} (m(\nu_k)+\alpha)\|k\|^{n-\beta} = C_1,$$

which implies that for any $\varepsilon > 0$,

$$\frac{C_1(1-\varepsilon)}{\|k\|^{n-\beta}} < m(\nu_k)+\alpha < \frac{C_1(1+\varepsilon)}{\|k\|^{n-\beta}},$$

for sufficiently large $\|k\|$. Thus

$$\|k\|^{n-\beta}\left(1-e^{-\frac{C_1(1-\varepsilon)t}{\|k\|^{n-\beta}}}\right) < \|k\|^{n-\beta}\left(1-e^{-(m(\nu_k)+\alpha)t}\right) < \|k\|^{n-\beta}\left(1-e^{-\frac{C_1(1+\varepsilon)t}{\|k\|^{n-\beta}}}\right),$$

and consequently,

$$C_1(1-\varepsilon)t < \lim_{\|k\|\to\infty} \|k\|^{n-\beta}\left(1-e^{-(m(\nu_k)+\alpha)t}\right) < C_1(1+\varepsilon)t.$$

Since ε is arbitrary, we obtain

$$\lim_{\|k\|\to\infty} \|k\|^{n-\beta}\left(1-e^{-(m(\nu_k)+\alpha)t}\right) = C_1 t,$$

and thus,

$$\left(1-e^{-(m(\nu_k)+\alpha)t}\right)e^{m(\nu_k)t} \sim \frac{C_1 t e^{-\alpha t}}{\|k\|^{n-\beta}}.$$

The proof is similar for the case $\beta \leq \frac{n-1}{2}$. $\square$

Conditions on f and β to guarantee the continuity of v, the solution of (2.22), are given in the following result.

Theorem 2.7. *Let $v(x,t)$ be as in (2.23) and assume that $\hat{f}_k$ satisfies*

$$\hat{f}_k \sim \begin{cases} \frac{1}{\|k\|^{\beta+\varepsilon}}, & \text{if } \frac{n-1}{2} < \beta < n, \\ \frac{1}{\|k\|^{\frac{n-1}{2}+\zeta}}, & \text{if } \beta \leq \frac{n-1}{2}, \end{cases}$$

for $\varepsilon, \zeta > 0$. Then, $v(x,t)$ is continuous.

Proof. For $\frac{n-1}{2} < \beta < n$ with $\hat{f}_k \sim \frac{1}{\|k\|^{\beta+\varepsilon}}$, then by using Lemma 2.4, we have

$$\hat{v}_k = \hat{f}_k \left(1 - e^{-(m(\nu_k)+\alpha)t}\right) e^{m(\nu_k)t} \sim \frac{Cte^{-\alpha t}}{\|k\|^{n+\varepsilon}}.$$

Similarly, for $\beta \leq \frac{n-1}{2}$ with $\hat{f}_k \sim \frac{1}{\|k\|^{\frac{n-1}{2}+\zeta}}$, then

$$\hat{v}_k = \hat{f}_k \left(1 - e^{-(m(\nu_k)+\alpha)t}\right) e^{m(\nu_k)t} \sim \frac{Cte^{-\alpha t}}{\|k\|^{n+\zeta}}.$$

By Proposition 3.3.12 in [27], we conclude that for $t > 0$, $v(\cdot, t)$ is continuous in both cases. $\square$

The following theorem summarizes the results in this section.

Theorem 2.8. *Let $\beta < n$ and let u be as given in (2.23) and assume that*

$$\hat{f}_k \sim \begin{cases} \frac{1}{\|k\|^{\beta+\varepsilon}}, & \text{if } \frac{n-1}{2} < \beta < n, \\ \frac{1}{\|k\|^{\frac{n-1}{2}+\zeta}}, & \text{if } \beta \leq \frac{n-1}{2}, \end{cases}$$

for some $\varepsilon, \zeta > 0$. Then, if f is discontinuous at x then u is discontinuous at x.

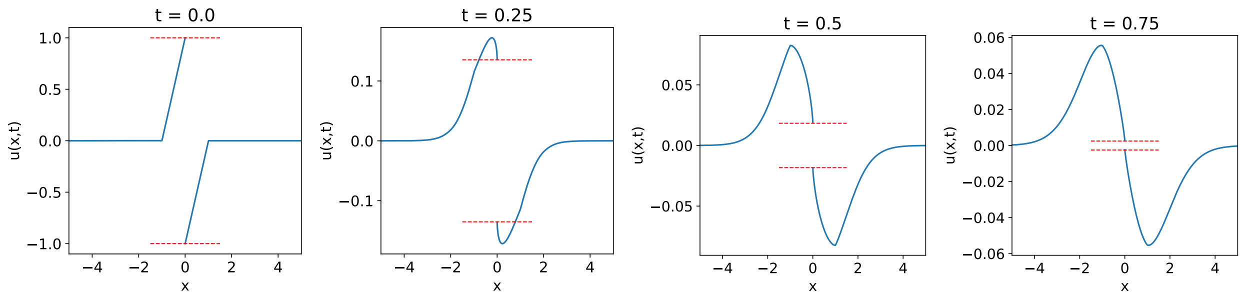

Figure 2.1: The slow decay of a discontinuity in the nonlocal diffusion equation with $\beta < n$.

Corollary 2.1. *If $f \in L^2(T)$ is piecewise continuous, then u is piecewise continuous and f and u share the same locations of jumps. Furthermore, the magnitude of a jump decays as t increases.*

This is an immediate consequence of Theorem 2.8, since for a piecewise continuous function $f \in L^2(T)$, we have $\hat{f}_k \sim \dfrac{C}{|k|}$, for some $C > 0$.

A one-dimensional example for the propagation of a discontinuity in the nonlocal diffusion equation is described below. Figure 2.1 shows the results of a numerical solution to the periodic nonlocal diffusion problem $u_t = \mathcal{L}^{\delta,\beta}u$ on the interval $(-10, 10)$ with $\delta = 1$, $\beta = 1/3$, and initial condition

$$u(x,0) = \begin{cases} x+1 & \text{if } -1 < x \leq 0, \\ x-1 & \text{if } 0 < x < 1, \\ 0 & \text{otherwise.} \end{cases}$$

In Figure 2.1, function values for $x < 0$ were plotted separately from those for $x > 0$ so that the jump is apparent. The dashed lines indicate the values $\pm e^{-\alpha t}$, showing the theoretical extremes of the jump.

Chapter 3

Regularity of solutions for nonlocal diffusion equation with a diffusion source

In this chapter, we focus on the following nonlocal diffusion equation with a diffusion source and zero initial data

$$\begin{cases} u_t(x,t) = \mathcal{L}^{\delta,\beta} u(x,t) + b(x), \;\; x \in T^n, \;\; t > 0, \\ u(x,0) = 0. \end{cases} \tag{3.1}$$

To study the existence, uniqueness, and regularity of solutions to nonlocal diffusion equations over the space of periodic distributions, we consider the identification $U(t) = u(\cdot, t)$, with $U : [0, \infty) \to H^s(T^n)$.

Let $b \in H^s(T^n)$ and define $U, V : [0, \infty) \to H^q(T^n)$ for some $q \in \mathbb{R}$, by

$$U(t) \;\; = \;\; \hat{b}_0 t + \sum_{0 \neq k \in \mathbb{Z}^n} \frac{e^{m(\nu_k)t} - 1}{m(\nu_k)} \hat{b}_k e^{i\nu_k \cdot x}, \tag{3.2}$$

$$V(t) \;\; = \;\; \sum_{k \in \mathbb{Z}^n} e^{m(\nu_k)t} \hat{b}_k e^{i\nu_k \cdot x}. \tag{3.3}$$

Observe that for any $t \geq 0$, $U(t)$ and $V(t)$ are well-defined periodic distributions, since $\frac{e^{m(\nu_k)t}-1}{m(\nu_k)}$ and $e^{m(\nu_k)t}$ are bounded functions in k.

Theorem 3.1. *Let $n \geq 1$, $\delta > 0$, and $\beta < n+4$. Assume that $\varepsilon_1 > 0$ and $b \in H^s(T^n)$ for some $s \in \mathbb{R}$. Then for any fixed $t > 0$, $U(t) \in H^p(T^n)$ and $V(t) \in H^r(T^n)$, where*

$$p = \begin{cases} s, & \text{if } \beta \leq n, \\ s+\beta-n, & \text{if } \beta > n, \end{cases} \qquad \text{and} \qquad r = \begin{cases} s, & \text{if } \beta < n, \\ s + \dfrac{4nt}{\delta^2}(1-\varepsilon_1), & \text{if } \beta = n, \\ \infty, & \text{if } \beta > n. \end{cases} \tag{3.4}$$

Proof. We observe that

$$\begin{aligned} \|U(t) - \hat{b}_0 t\|^2_{H^p(T^n)} &= \sum_{0 \neq k \in \mathbb{Z}^n} (1+\|k\|^2)^p |\hat{U}_k(t)|^2 \\ &= \sum_{0 \neq k \in \mathbb{Z}^n} \frac{(1+\|k\|^2)^{p-s}}{|m(\nu_k)|^2} (e^{m(\nu_k)} - 1)^2 (1+\|k\|^2)^s |\hat{b}_k|^2. \end{aligned}$$

Since $b \in H^s(T^n)$ and $e^{m(\nu_k)t}$ is bounded because $m(\nu_k) < 0$, then the result follows by showing that

$$\frac{(1+\|k\|^2)^{p-s}}{|m(\nu_k)|^2},$$

is bounded for $k \neq 0$. When $\beta \leq n$, then $p - s = 0$ and by using Theorem 1.2, there exist $C_1 > 0$ and $r_1 > 0$ such that $|m(\nu_k)| \geq C_1$, for all $\|k\| \geq r_1$. Thus,

$$\frac{(1+\|k\|^2)^{p-s}}{|m(\nu_k)|^2} \leq \frac{1}{C_1^2}.$$

When $\beta > n$, then $p - s = \beta - n$, and by using Theorem 1.2, there exist $C_2 > 0$ and $r_2 > 0$ such that $|m(\nu_k)| \geq C_2 \|k\|^{\beta-n}$, for all $\|k\| \geq r_2$. This implies that

$$\frac{(1+\|k\|^2)^{p-s}}{|m(\nu_k)|^2} \leq \frac{1}{C_2^2} \left(\frac{1+\|k\|^2}{\|k\|^2} \right)^{\beta-n},$$

which is bounded. The proof of $V(t) \in H^r(T^n)$ is similar to the proof of Theorem 2.1. $\square$

Lemma 3.1. *Let U and V be as defined in (3.2) and (3.3), respectively. Then*

$$V(t) = \mathcal{L}^{\delta,\beta}U(t) + b.$$

Proof. By using (2.11), for any $x \in T^n$ and $t > 0$, we have

$$\begin{aligned}
\mathcal{L}^{\delta,\beta}U(t)(x) &= \mathcal{L}^{\delta,\beta}(\hat{b}_0 t) + \sum_{0\neq k\in\mathbb{Z}^n} m(\nu_k)\hat{U}_k(t)e^{i\nu_k\cdot x} \\
&= \sum_{0\neq k\in\mathbb{Z}^n} m(\nu_k)\frac{(e^{m(\nu_k)t}-1)}{m(\nu_k)}\hat{b}_k e^{i\nu_k\cdot x} \\
&= \sum_{0\neq k\in\mathbb{Z}^n} \hat{b}_k e^{m(\nu_k)t}e^{i\nu_k\cdot x} - \sum_{0\neq k\in\mathbb{Z}^n} \hat{b}_k e^{i\nu_k\cdot x} \\
&= V(t)(x) - b(x).
\end{aligned}$$

□

Proposition 3.1. *Let $U(t)$ and $V(t)$ be as defined in (3.2) and (3.3), respectively. Then,*

$$\frac{dU}{dt} = V(t).$$

Moreover, for $N \geq 1$,

$$\frac{d^N U}{dt^N} = \sum_{k\in\mathbb{Z}^n} \hat{b}_k m(\nu_k)^{N-1} e^{m(\nu_k)t} e^{i\nu_k\cdot x},$$

for all $t \in (0,\infty)$, where the differentiation here is in the sense of Gateaux differentiation.

Proof. We show that

$$\lim_{h\to 0}\left\| \frac{1}{h}\left[U(t+h) - U(t)\right] - V(t)\right\|^2_{H^q(T^n)} = 0,$$

where $q = s$ when $\beta \leq n$ and q is arbitrary when $\beta > n$. Equivalently, we show that

$$\lim_{h\to 0}\sum_{0\neq k\in\mathbb{Z}^n}(1+\|k\|^2)^q|\hat{b}_k|^2\left[\frac{1}{h}\left(e^{m(\nu_k)h}-1\right)\frac{e^{m(\nu_k)t}}{m(\nu_k)} - e^{m(\nu_k)t}\right]^2 = 0. \tag{3.5}$$

This result follows from passing the limit inside the sum, which we justify next by the dominated convergence theorem.

When $\beta < n$, then $q = s$ and similar to (2.13), there exists a constant $C_2 > 0$ such that

$$\left| \frac{e^{m(\nu_k)h} - 1}{h} \right| < C_2,$$

for all k, and for sufficiently small h. Moreover, $e^{m(\nu_k)t}$ and $\frac{1}{m(\nu_k)}$, for $k \neq 0$, are bounded. Combining this with the fact that $b \in H^s(T^n)$, it follows that the summand in the left hand side of (3.5) is uniformly bounded.

For the cases $\beta > n$ and $\beta = n$, we first note that the summand in (3.5) can be written as

$$(1 + \|k\|^2)^s |b_k|^2 (1 + \|k\|^2)^{q-s} \frac{e^{2m(\nu_k)t}}{m(\nu_k)^2} \left(\frac{e^{m(\nu_k)} - 1 - m(\nu_k)h}{h} \right)^2 .$$

Since $b \in H^s(T^n)$, then it is left to show that

$$(1 + \|k\|^2)^{q-s} \frac{e^{2m(\nu_k)t}}{m(\nu_k)^2} \left(\frac{e^{m(\nu_k)} - 1 - m(\nu_k)h}{h} \right)^2 \tag{3.6}$$

is uniformly bounded. Using (2.15), we have

$$(1 + \|k\|^2)^{q-s} \frac{e^{2m(\nu_k)t}}{m(\nu_k)^2} \left(\frac{e^{m(\nu_k)} - 1 - m(\nu_k)h}{h} \right)^2 \leq \frac{1}{4} (1 + \|k\|^2)^{q-s} m(\nu_k)^2 e^{2m(\nu_k)t}.$$

When $\beta = n$, then $q - s = 0$ and since $m(\nu_k) \to -\infty$ as $\|k\| \to \infty$, then

$$\frac{1}{4} m(\nu_k)^2 e^{2m(\nu_k)t} \to 0$$

as $\|k\| \to \infty$ showing that (3.6) is uniformly bounded.

When $\beta > n$, then by using Theorem 1.2, we have that

$$\frac{1}{4} (1 + \|k\|^2)^{q-s} m(\nu_k)^2 e^{2m(\nu_k)t} = \frac{(1 + \|k\|^2)^{q-s} m(\nu_k)^2}{4 e^{2|m(\nu_k)|t}} \to 0$$

as $\|k\| \to \infty$, showing that (3.6) is uniformly bounded and therefore completing the proof of the first part.

The second part of this proposition follows from arguments similar to those in the proof of Proposition 2.1. $\square$

The following regularity theorem summarizes the results of this subsection.

Theorem 3.2. *Let $b \in H^s(T^n)$ with $s \in \mathbb{R}$. Then there exists a unique solution U to the nonlocal diffusion equation*

$$\begin{cases} \dfrac{dU}{dt} = \mathcal{L}^{\delta,\beta} U(t) + b, \\ U(0) = 0. \end{cases} \tag{3.7}$$

Moreover, $U \in C^\infty((0,\infty); H^p(T^n))$, where p is as defined in (3.4).

Remark 3.1. *The temporal regularity is in the sense of Gateaux differentiation.*

Proof. The existence follows from Lemma 3.1 and Proposition 3.1. For the uniqueness, the proof is similar to the proof of uniqueness in Theorem 2.2. The spatial regularity follows from Theorem 3.1 and the temporal regularity follows from Proposition 3.1. $\square$

3.1 Regular functions as solutions of nonlocal diffusion equation with diffusion source

In this section, we focus on functions b with absolutely summable Fourier coefficients, $\sum_{k\in\mathbb{Z}^n} |\hat{b}_k| < \infty$.

Proposition 3.2. *Let $b \in H^s(T^n)$ such that $\sum_{k\in\mathbb{Z}^n} |\hat{b}_k| < \infty$ and let $\beta < n+4$. Then*

$$u(x,\cdot) \in C^\infty((0,\infty)),$$

for all $x \in T^n$.

Proof. We use the Leibniz rule to differentiate under the sum. Let $g_k(t) = \frac{e^{m(\nu_k)t}-1}{m(\nu_k)}\hat{b}_k e^{i\nu_k\cdot x}$ and consider

$$\begin{aligned}
\sum_{0\neq k\in\mathbb{Z}^n} |g_k(t)| &= \sum_{0\neq k\in\mathbb{Z}^n} \left|\frac{e^{m(\nu_k)t}-1}{m(\nu_k)}\hat{b}_k e^{i\nu_k\cdot x}\right| \\
&= \sum_{0\neq k\in\mathbb{Z}^n} |\hat{b}_k| \left|\frac{e^{m(\nu_k)t}-1}{m(\nu_k)}\right| \\
&\leq \sum_{0\neq k\in\mathbb{Z}^n} |\hat{b}_k| \frac{1}{|m(\nu_k)|},
\end{aligned}$$

where in the last inequality, we used the fact that $m(\nu_k) < 0$. Since $\frac{1}{|m(\nu_k)|}$, $k \neq 0$, is bounded and $\sum_{k\in\mathbb{Z}^n} |\hat{b}_k| < \infty$, then $g_k(t)$ is summable for any fixed t. Moreover,

$$\frac{dg_k}{dt} = \hat{b}_k e^{m(\nu_k)t} e^{i\nu_k\cdot x},$$

is continuous for all k. Now fix $t > 0$, then there exists τ such that $0 < \tau < t$. We define $\theta_k := |\hat{b}_k| e^{m(\nu_k)\tau}$. Since $m(\nu_k) \leq 0$, for all k, then

$$\theta_k = |\hat{b}_k| e^{m(\nu_k)\tau} \leq |\hat{b}_k|,$$

showing that θ_k is summable. Moreover,

$$\left|\frac{dg_k}{dt}\right| = |\hat{b}_k| e^{m(\nu_k)t} \leq |\hat{b}_k| e^{m(\nu_k)\tau} = \theta_k.$$

Therefore,

$$\begin{aligned}
\frac{\partial u(x,t)}{\partial t} &= \hat{b}_0 + \frac{d}{dt}\sum_{0\neq k\in\mathbb{Z}^n} g_k(t) \\
&= \hat{b}_0 + \sum_{0\neq k\in\mathbb{Z}^n} \frac{dg_k}{dt} \\
&= \sum_{k\in\mathbb{Z}^n} \hat{b}_k e^{m(\nu_k)t} e^{i\nu_k\cdot x}.
\end{aligned}$$

This shows that u is differentiable with respect to t. For higher derivatives, let $N \geq 2$ be an integer, we observe that

$$\frac{d^N g_k}{dt^N} = \hat{b}_k \ (m(\nu_k))^{N-1} e^{m(\nu_k)t} e^{i\nu_k \cdot x}.$$

Define $\theta_k = |\hat{b}_k||m(\nu_k)|^{N-1} e^{m(\nu_k)\tau}$. When $\beta < n$, then there exists $C > 0$ such that $|m(\nu_k)| \leq C$. Thus,

$$\theta_k = |\hat{b}_k||m(\nu_k)|^{N-1} e^{m(\nu_k)\tau} \leq C^{N-1} |\hat{b}_k|,$$

showing that θ_k is summable. When $\beta \geq n$, then $e^{m(\nu_k)\tau} \to 0$ as $\|k\| \to \infty$. Thus, $|m(\nu_k)|^{N-1} e^{m(\nu_k)\tau} \leq 1$ for sufficiently large $\|k\|$. Hence $\theta_k \leq |\hat{b}_k|$, showing that θ_k is summable. Furthermore,

$$\left| \frac{d^N g_k}{dt^N} \right| = |\hat{b}_k||m(\nu_k)|^{N-1} e^{m(\nu_k)t} \leq |\hat{b}_k||m(\nu_k)|^{N-1} e^{m(\nu_k)\tau} = \theta_k.$$

This implies that $u(x, \cdot)$ is N-times continuously differentiable and

$$\begin{aligned} \frac{\partial^N u(x,t)}{\partial t^N} &= \frac{d^N}{dt^N} \sum_{k \in \mathbb{Z}^n} g_k(t) \\ &= \sum_{k \in \mathbb{Z}^n} \frac{d^N g_k}{dt^N} \\ &= \sum_{k \in \mathbb{Z}^n} \hat{b}_k |m(\nu_k)|^{N-1} e^{m(\nu_k)t} e^{i\nu_k \cdot x}. \end{aligned}$$

Since N is arbitrary, it follows that $u(x, \cdot) \in C^\infty((0, \infty))$. □

From Theorem 3.1 and Proposition 3.2 we obtain the following regularity result.

Theorem 3.3. *Let $n \geq 1$, $\delta > 0$ and $\beta < n + 4$. Assume that $b \in H^s(T^n)$ and its Fourier coefficients are summable. Then,*

1. *$u \in C^\infty((0, \infty); H^s(T^n))$, for $\beta \leq n$,*
2. *$u \in C^\infty\left((0, \infty); H^{s+\beta-n}(T^n)\right)$, for $\beta > n$.*

Convergence of solutions of the nonlocal diffusion equation (3.1) to the solution of the corresponding classical diffusion equation is given next in Theorem 3.4 and Theorem 3.5.

Theorem 3.4. *Let $n \geq 1$ and $b \in H^s(T^n)$, with $s \in \mathbb{R}$. Suppose u is the solution of the classical diffusion equation $u_t = \triangle u + b$ with initial condition $u|_{t=0} = 0$. For any $\delta > 0$, let $u^{\delta,\beta}$ be the solution of the nonlocal diffusion equation*

$$\begin{cases} u_t^{\delta,\beta}(x,t) = \mathcal{L}^{\delta,\beta} u^{\delta,\beta}(x,t) + b(x), \;\; x \in T^n, \;\; t > 0, \\ u^{\delta,\beta}(x,0) = 0, \;\; x \in T^n. \end{cases} \tag{3.8}$$

Then, for $t > 0$ and $\beta \leq n$,

$$\lim_{\delta \to 0^+} u^{\delta,\beta}(\cdot,t) = u(\cdot,t), \quad \text{in } H^s(T^n),$$

and for $n < \beta \leq n+2$,

$$\lim_{\delta \to 0^+} u^{\delta,\beta}(\cdot,t) = u(\cdot,t), \quad \text{in } H^{s+\beta-n}(T^n).$$

Proof. The Fourier coefficients satisfy $\hat{u}_k^{\delta,\beta} = \frac{(e^{m(\nu_k)t}-1)}{m(\nu_k)} \hat{b}_k$ and $\hat{u}_k = \frac{(e^{-\|\nu_k\|^2 t}-1)}{-\|\nu_k\|^2} \hat{b}_k$, for $k \neq 0$. For $\beta \leq n$, then

$$\begin{aligned} \|u^{\delta,\beta}(\cdot,t) - u(\cdot,t)\|_{H^s(T^n)}^2 &= \sum_{0 \neq k \in \mathbb{Z}^n} (1+\|k\|^2)^s \; |\hat{u}_k^{\delta,\beta} - \hat{u}_k|^2 \\ &= \sum_{0 \neq k \in \mathbb{Z}^n} (1+\|k\|^2)^s \; \left| \frac{(e^{m(\nu_k)t}-1)}{m(\nu_k)} - \frac{(e^{-\|\nu_k\|^2 t}-1)}{-\|\nu_k\|^2} \right|^2 \; |\hat{b}_k|^2. \end{aligned}$$

To pass the limit $\delta \to 0^+$ inside the sum, it is sufficient to show that $\left| \frac{(e^{m(\nu_k)t}-1)}{m(\nu_k)} - \frac{(e^{-\|\nu_k\|^2 t}-1)}{-\|\nu_k\|^2} \right|$ is uniformly bounded. Using (1.4), $m(\nu) \leq 0$ for $\nu \in \mathbb{R}^n$, and thus,

$$\left| \frac{(e^{m(\nu_k)t}-1)}{m(\nu_k)} - \frac{(e^{-\|\nu_k\|^2 t}-1)}{-\|\nu_k\|^2} \right| \;\; \leq \;\; \frac{1}{|m(\nu_k)|} + \frac{1}{\|\nu_k\|^2}.$$

Since $\frac{1}{m(\nu_k)}$, $k \neq 0$, and $\frac{1}{\|\nu_k\|^2}$, $k \neq 0$, are bounded, then $\left| \frac{(e^{m(\nu_k)t}-1)}{m(\nu_k)} - \frac{(e^{-\|\nu_k\|^2 t}-1)}{-\|\nu_k\|^2} \right|$ is uniformly bounded. For the case $\beta > n$, consider

$$\begin{aligned}
\|u^{\delta,\beta}(\cdot,t) - u(\cdot,t)\|^2_{H^{s+\beta-n}(T^n)} &= \sum_{0\neq k\in\mathbb{Z}^n} (1+\|k\|^2)^{s+\beta-n}\ |\hat{u}^{\delta,\beta}_k - \hat{u}_k|^2 \\
&= \sum_{0\neq k\in\mathbb{Z}^n} (1+\|k\|^2)^{s}(1+\|k\|^2)^{\beta-n}\ \left|\frac{(e^{m(\nu_k)t}-1)}{m(\nu_k)} \right. \\
&\qquad \left. - \frac{(e^{-\|\nu_k\|^2 t}-1)}{-\|\nu_k\|^2}\right|^2 |\hat{b}_k|^2.
\end{aligned}$$

Since $(1+\|k\|^2)^s|\hat{b}_k|^2$ is summable, then to pass the limit inside the above sum, we show that the following function in k that is given by

$$(1+\|k\|^2)^{\beta-n}\ \left|\frac{(e^{m(\nu_k)t}-1)}{m(\nu_k)} - \frac{(e^{-\|\nu_k\|^2 t}-1)}{-\|\nu_k\|^2}\right|^2$$

is uniformly bounded. Since $m(\nu) \leq 0$ for all $\nu \in \mathbb{R}^n$, then

$$(1+\|k\|^2)^{\beta-n}\ \left|\frac{(e^{m(\nu_k)t}-1)}{m(\nu_k)} - \frac{(e^{-\|\nu_k\|^2 t}-1)}{-\|\nu_k\|^2}\right|^2 \ \leq\ (1+\|k\|^2)^{\beta-n}\ \left(\frac{1}{|m(\nu_k)|} + \frac{1}{\|\nu_k\|^2}\right)^2.$$

By using Theorem 1.2, there exists constant $C > 0$ such that $|m(\nu_k)| > C\|k\|^{\beta-n}$. Furthermore, using the fact that $A\|k\| \leq \|\nu_k\| \leq B\|k\|$ for positive constants A and B and since $\beta - n \leq 2$, then $\|\nu_k\|^2 \geq A^2\|k\|^{\beta-n}$. Therefore,

$$\begin{aligned}
(1+\|k\|^2)^{\beta-n}\ \left(\frac{1}{|m(\nu_k)|} + \frac{1}{\|\nu_k\|^2}\right)^2 &\leq (1+\|k\|^2)^{\beta-n}\left(\frac{1}{C\|k\|^{\beta-n}} + \frac{1}{A^2\|k\|^{\beta-n}}\right)^2 \\
&\leq \max\left(\frac{1}{C^2},\frac{1}{A^4}\right)\left(\frac{1+\|k\|^2}{\|k\|^2}\right)^{\beta-n},
\end{aligned}$$

showing uniform boundedness. Whether $\beta \leq n$ or $n < \beta \leq n+2$, we have $\lim_{\delta\to 0^+} m(\nu_k) = -\|\nu_k\|^2$, which implies that

$$\lim_{\delta\to 0^+}\|u^{\delta,\beta}(\cdot,t) - u(\cdot,t)\|_{H^s(T^n)} = 0,\ \text{ or }\ \lim_{\delta\to 0^+}\|u^{\delta,\beta}(\cdot,t) - u(\cdot,t)\|_{H^{s+\beta-n}(T^n)} = 0,$$

respectively, and therefore completing the proof. $\square$

A proof of the following lemma on the monotonicity of the multipliers can be found in [17].

Lemma 3.2. *Let $\beta' < \beta \le n+2$. Then, for all $\nu \neq 0$, $m^{\delta,\beta}(\nu) < m^{\delta,\beta'}(\nu)$.*

Theorem 3.5. *Let $n \ge 1, s \in \mathbb{R}$ and let $b \in H^s(T^n)$. Suppose u is the solution of the classical diffusion equation $u_t = \Delta u + b$, with $u|_{t=0} = 0$, and for any $\beta < n+2$, let $u^{\delta,\beta}$ be the solution of the nonlocal diffusion equation (3.8). Then, for $t > 0$, $\delta > 0$, and $0 < \varepsilon < 2$,*

$$\lim_{\beta \to (n+2)^-} u^{\delta,\beta}(\cdot,t) = u(\cdot,t), \ \textit{in } H^{s+2-\varepsilon}(T^n).$$

Proof. For $0 < \varepsilon < 2$, define $\beta' = n+2-\varepsilon$. For any $\beta > \beta'$, we have from Theorem 3.1 that $u^{\delta,\beta} \in H^{s+\beta-n}(T^n) \subset H^{s+2-\varepsilon}(T^n)$. Furthermore, $u \in H^{s+2}(T^n) \subset H^{s+2-\varepsilon}(T^n)$. Thus the limit makes sense. Consider

$$\begin{aligned}\|u^{\delta,\beta}(\cdot,t) - u(\cdot,t)\|^2_{H^{s+2-\varepsilon}(T^n)} &= \sum_{0\neq k \in \mathbb{Z}^n} (1+\|k\|^2)^{2-\varepsilon} \left| \frac{e^{m^{\delta,\beta}(\nu_k)t} - 1}{m^{\delta,\beta}(\nu_k)} \right. \\ &\qquad \left. - \frac{e^{-\|\nu_k\|^2 t} - 1}{-\|\nu_k\|^2} \right|^2 (1+\|k\|^2)^s \|\hat{b}_k\|^2.\end{aligned}$$

Since $b \in H^s(T^n)$, in order to pass the limit in β inside the sum, we show that the expression

$$(1+\|k\|^2)^{2-\varepsilon} \left| \frac{e^{m^{\delta,\beta}(\nu_k)t} - 1}{m^{\delta,\beta}(\nu_k)} - \frac{e^{-\|\nu_k\|^2 t} - 1}{-\|\nu_k\|^2} \right|^2$$

is uniformly bounded for $k \neq 0$ and $\beta \in [\beta', n+2)$. Applying Lemma 3.2,

$$\begin{aligned}(1+\|k\|^2)^{2-\varepsilon} \left| \frac{e^{m^{\delta,\beta}(\nu_k)t} - 1}{m^{\delta,\beta}(\nu_k)} - \frac{e^{-\|\nu_k\|^2 t} - 1}{-\|\nu_k\|^2} \right|^2 &\le (1+\|k\|^2)^{2-\varepsilon} \left(\frac{1}{|m^{\delta,\beta}(\nu_k)|} + \frac{1}{\|\nu_k\|^2} \right)^2 \\ &\le (1+\|k\|^2)^{2-\varepsilon} \left(\frac{1}{|m^{\delta,\beta'}(\nu_k)|} + \frac{1}{\|\nu_k\|^2} \right)^2.\end{aligned}$$

From Theorem 1.2, there exists $C > 0$ such that $|m^{\delta,\beta'}(\nu_k)| \ge C\|k\|^{2-\varepsilon}$. Furthermore, there exists $A > 0$ such that $\|\nu_k\| \geq A\|k\|$. Thus,

$$\begin{aligned}(1+\|k\|^2)^{2-\varepsilon}\left(\frac{1}{|m^{\delta,\beta'}(\nu_k)|}+\frac{1}{\|\nu_k\|^2}\right)^2 &\leq (1+\|k\|^2)^{2-\varepsilon}\left(\frac{1}{C\|k\|^{2-\varepsilon}}+\frac{1}{A^2\|k\|^2}\right)^2\\ &\leq (1+\|k\|^2)^{2-\varepsilon}\left(\frac{1}{C\|k\|^{2-\varepsilon}}+\frac{1}{A^2\|k\|^{2-\varepsilon}}\right)^2,\end{aligned}$$

which is uniformly bounded. Since $\lim_{\beta\to(n+2)^-} m(\nu_k) = -\|\nu_k\|^2$, then the result follows. $\square$

Chapter 4

Two dimensional Fourier continuation

In this chapter, we provide a description of the two-dimensional Fourier continuation (2D-FC) following the algorithm presented in [2]. The 2D-FC method is used for constructing a periodic extension of a smooth nonperiodic 2D function defined on a smooth two-dimensional domain. This algorithm executes at a computational cost of $\mathcal{O}(N \log N)$ for an N-point discretization grid and converges with a specified dth order of convergence.

4.1 1D blending-to-zero algorithm

In the description given in [28], the 1D blending-to-zero algorithm starts by smoothly extending the vector $f = (f_1, f_2, \ldots, f_N) \in \mathbb{R}^N$ of values of a complex-valued function f over the set of uniformly spaced nodes $\mathcal{D} = \{x_1, x_2, \ldots, x_N\}$ where for a given step size $h > 0$,

$$x_j = x_1 + (j-1)h.$$

Without loss of generality, we assume that $x_1 = 0$ and $x_N = 1$. The extension, which relies on some number d of near-boundary function values $\{f_1, f_2, \ldots, f_d\}$ near $x = 0$ and $\{f_{N-d+1}, f_{N-d+2}, \ldots, f_N\}$ near $x = 1$, produces a sequence $\{\tilde{f}_j\}_{j=-\infty}^{\infty}$ with the property that $\tilde{f}_j = f_j$ for $j = 1, 2, \ldots, N$. The extended vector $\tilde{f}$ is then blended to zero on either end by multiplying with a suitable windowing function. This algorithm is depicted in Figure 4.1d and is briefly summarized below:

Let p_l and p_r be the unique, lowest degree polynomials such that p_l interpolates $\{(x_j, f_j)\}_{j=1}^{d}$ and p_r interpolates $\{(x_j, f_j)\}_{j=N-d+1}^{N}$. Define the extension $\{\tilde{f}_j\}$ as follows

$$\tilde{f}_j = \begin{cases} p_l(x_j), & \text{if } j < 1, \\ f_j, & \text{if } 1 \leq j \leq N, \\ p_r(x_j), & \text{if } j > N. \end{cases}$$

For convenience, we can represent this operation in a matrix form using the following two Vandermonde matrices

$$A_l = \begin{pmatrix} 1 & x_1 & x_1^2 & \dots & x_1^{d_l-1} \\ 1 & x_2 & x_2^2 & \dots & x_2^{d_l-1} \\ \vdots & \vdots & \vdots & \ddots & \vdots \\ 1 & x_{d_l} & x_{d_l}^2 & \dots & x_{d_l}^{d_l-1} \end{pmatrix} \text{ and } B_l = \begin{pmatrix} 1 & x_{1-M} & x_{1-M}^2 & \dots & x_{1-M}^{d_l-1} \\ 1 & x_{2-M} & x_{2-M}^2 & \dots & x_{2-M}^{d_l-1} \\ \vdots & \vdots & \vdots & \ddots & \vdots \\ 1 & x_0 & x_0^2 & \dots & x_0^{d_l-1} \end{pmatrix}.$$

Then for any vector $v \in \mathbb{R}^{d_l}$, $A_l^{-1}v$ contains the coefficients of the polynomial interpolant of the points $\{(x_i, v_i)\}_{i=1}^{d_l}$ in order of increasing degree, and $B_l A_l^{-1} v$ contains the values of the same interpolating polynomial at the points $\{x_i\}_{i=1-M}^{0}$ (for the leftward extension). Let $A_l = Q_l R_l$ be the QR factorization of A_l and define $E_l = B_l R_l^{-1}$. Then, we have that $B_l A_l^{-1} = E_l Q_l^T$. We can do the same operation at the right endpoint to produce matrices E_r and Q_r. If we then write $f = (f_l^T, f_c^T, f_r^T)^T$, where $f_l \in \mathbb{R}^{d_l}$, $f_c \in \mathbb{R}^{N-d_l-d_r}$, and $f_r \in \mathbb{R}^{d_r}$, then the extension of f can be expressed as

$$\tilde{f} = \begin{pmatrix} E_l Q_l^T & 0 & 0 \\ I & 0 & 0 \\ 0 & I & 0 \\ 0 & 0 & I \\ 0 & 0 & E_r Q_r^T \end{pmatrix} \begin{pmatrix} f_l \\ f_c \\ f_r \end{pmatrix}.$$

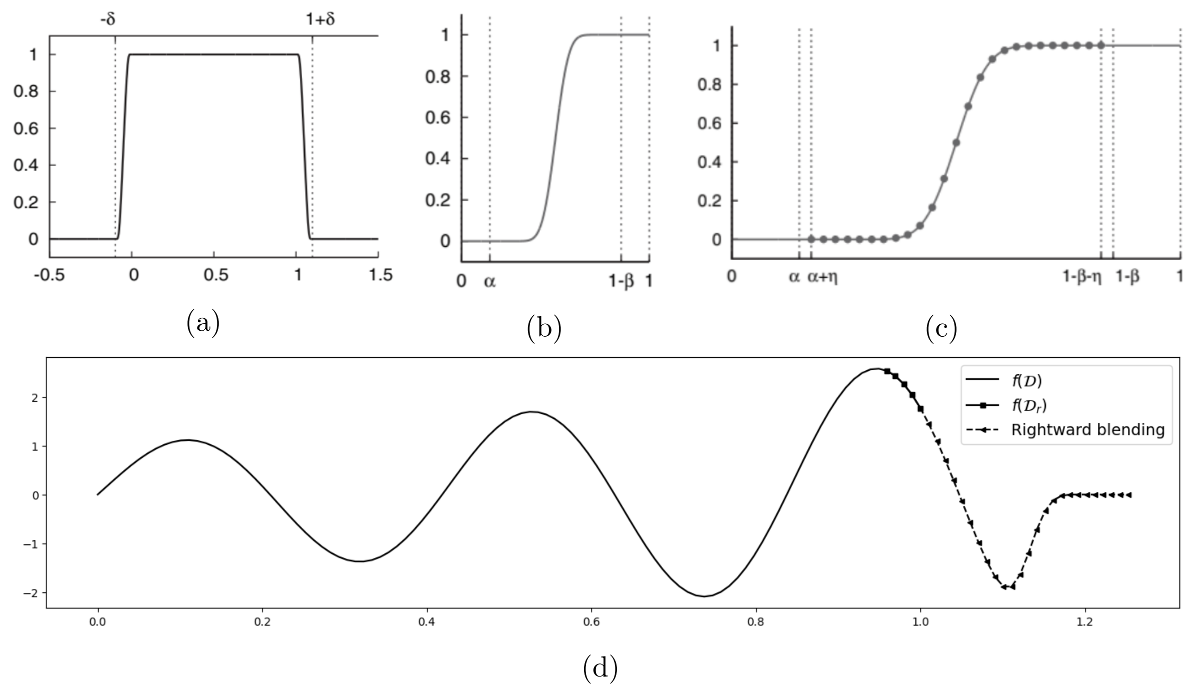

Figure 4.1: In (a), a smooth and symmetric windowing function. In (b), a smooth step function transitioning between the values 0 and 1 at α and $1-\beta$, respectively. In (c), the sampling of the step at 25 equispaced nodes in the interval $(\alpha, 1-\beta)$. In (d), a demonstration of 1D blending to zero on a smooth but nonperiodic function $f(x) = \sin(15x)e^x$ on [0,1].

Finally, we blend the extended function $\tilde{f}$ to zero on either end by multiplying by a windowing function which is smooth and symmetric on both sides. The smooth window, as shown in Figure 4.1a, is determined by the smooth step-up in the transition region $[-\delta, 0]$ or $[1, 1+\delta]$. Let $\psi \in C^\infty([0,1])$ as shown in Figure 4.1b, with $0 \le \psi \le 1$, and

$$\psi(x) = 0, \text{ for } x \text{ in a neighborhood of } [0, \alpha]$$

$$\psi(x) = 1, \text{ for } x \text{ in a neighborhood of } [1-\beta, 1]$$

Then, such ψ generates a smooth step-up function on $[0,1]$ defined by

$$S(x) = \psi(\alpha(1-x) + (1-\beta)x).$$

The window function is then defined by

$$W(x;\delta) = \begin{cases} 0, & x \in (-\infty, -\delta) \cup (1+\delta, \infty), \\ 1, & x \in [0,1], \\ S(1+\frac{x}{\delta}), & x \in (-\delta, 0), \\ S(1-\frac{x-1}{\delta}), & x \in (1, 1+\delta). \end{cases}$$

We need M values of ψ sampled in the transition region $(\alpha, 1-\beta)$ in order to apply $W(x;\delta)$ to $\tilde{f}$. These samples are

$$\psi(\alpha + \eta j) \quad j = 1, 2, 3, \ldots, M \quad \text{where } \eta = \frac{1-\alpha-\beta}{M-1}, \tag{4.1}$$

and are shown in Figure 4.1c. After scaling and translation, the interval $(\alpha, 1-\beta)$ corresponds to the interval $(-\delta, 0)$ in Figure 4.1a and the step size η corresponds to the grid step size h. Therefore, the samples in (4.1) are the required samples of $W(x;\delta)$ in the transition region $(-\delta, 0)$. By multiplying these samples with the columns of E_l and E_r element-wise, we have the following discrete windowed extension operator

$$\tilde{f}_W = \begin{pmatrix} \widetilde{E}_l Q_l^T & 0 & 0 \\ I & 0 & 0 \\ 0 & I & 0 \\ 0 & 0 & I \\ 0 & 0 & \widetilde{E}_r Q_r^T \end{pmatrix} \begin{pmatrix} f_l \\ f_c \\ f_r \end{pmatrix},$$

where $\widetilde{E}_l$ and $\widetilde{E}_r$ are the counterparts of E_l and E_r respectively, blended to zero by ψ. A demonstration of the 1D blending to zero is shown in Figure 4.1d.

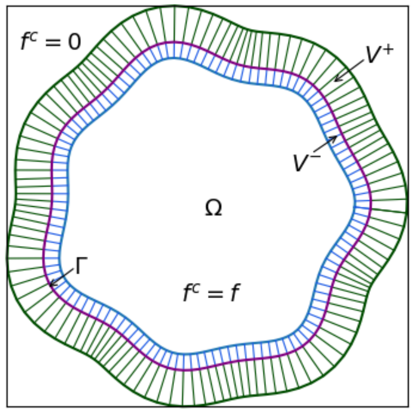

Figure 4.2: Geometric constructions of the 2D-FC procedure. The interior strip V^- and the exterior strip V^+ are defined in Section 4.2.1.

4.2 2D-FC algorithm

Let $f : \overline{\Omega} \to \mathbb{C}$ be given, where the domain $\Omega \subset \mathbb{R}^2$ has a smooth boundary $\Gamma = \overline{\Omega} \setminus \Omega$. We assume that the values of f are known on the uniform Cartesian grids within $\overline{\Omega}$ and on the grid points on the boundary. The algorithm first produces 1D blending to zero values for f along directions normals to the boundary Γ, to produce continuation values that vanish on a certain 2D tangential-normal curvilinear grid around Γ as depicted in Figure 4.2. These continuation values are then interpolated onto Cartesian grid points inside the region V^+ to produce a 2D blending to zero continuation of f. Once all the interpolated values have been obtained at all Cartesian grid points around Γ, the 2D-FC function is then obtained via a 2D Fast Fourier Transform (FFT) given by

$$f^c(x, y) = \sum_{k=\frac{N_x}{2}+1}^{N_x/2} \sum_{l=\frac{N_y}{2}+1}^{N_y/2} \hat{f}^c_{kl} \exp\left(\frac{2\pi i k x}{L_x}\right) \exp\left(\frac{2\pi i l y}{L_y}\right), \tag{4.2}$$

where L_x and L_y are the periods in x and y directions respectively.

4.2.1 Curvilinear grids along a 2D tangential-normal

The curvilinear grids are introduced within the interior and exterior strips V^- and V^+ respectively, as shown in Figure 4.2. These strips are given by

$$\begin{aligned} V^- &= \{q(\theta) - n(\theta)\gamma : 0 \leq \theta \leq 2\pi \text{ and } 0 \leq \gamma \leq (d-1)k_1\} \\ V^+ &= \{q(\theta) + n(\theta)\gamma : 0 \leq \theta \leq 2\pi \text{ and } 0 \leq \gamma \leq Ck_1\}, \end{aligned}$$

where $q(\theta) = (x(\theta), y(\theta))$ is the parametrization of Γ, $n(\theta) = (n_x(\theta), n_y(\theta))$ is the unit normal to the boundary at $q(\theta)$, and d, C, k_1 represent the number of matching points near the boundary, the number of continuation points, and the step size along the normals respectively. Consider the following uniform discretization of the interval $[0, 2\pi]$

$$\Theta_B = \{\theta_p = pk_2 : 0 \leq p < B,\ k_2 = 2\pi/B\}. \tag{4.3}$$

Then for each $\theta_p \in \Theta_B$, the curvilinear grid along the corresponding normal within V^- and V^+ are respectively given as

$$\begin{aligned} V^-_{\theta_p} &= \{r_{p,q} = q(\theta_p) + n(\theta_p)(q-d+1)k_1,\ 0 \leq q \leq d-1\} \\ V^+_{\theta_p} &= \{s_{p,q} = q(\theta_p) + n(\theta_p)qk_1/n_r,\ 0 \leq q \leq C_r\}, \end{aligned}$$

where $C_r = Cn_r$ for some integer refinement factor n_r (Remark 4.1). Let $\mathcal{R} = [a_0, a_1] \times [b_0, b_1]$ be the smallest closed rectangle which contains $\Omega \cup V^+$ as shown in Figure 4.2, and define the following Cartesian grid $\mathcal{H}$ on $\mathcal{R}$ with step size h, where the continuation function values will be computed.

$$\mathcal{H} = \{z_{ij} = (x_i, y_j) : x_i = a_0 + ih;\ y_j = b_0 + jh, 0 \leq i < N_x \text{ and } 0 \leq j < N_y\}.$$

Remark 4.1. *The refinement factor n_r helps to prevent accuracy loss by making the normal-direction grids at the exterior finer than the grids inherent by the blending-to-zero process.*

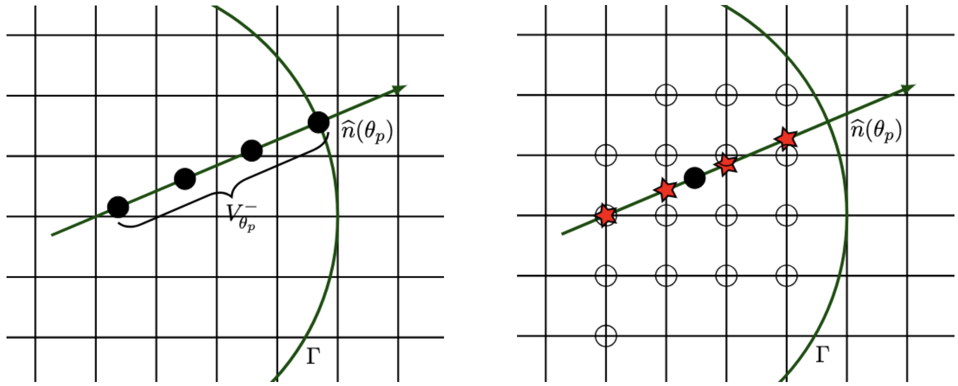

Figure 4.3: Interpolation procedure for evaluating values of f on the set $V^-_{\theta_p}$ for the case $|n_x(\theta_p)| \geq |n_y(\theta_p)|$. The black solid circles indicate the points that define the set $V^-_{\theta_p}$. The known values of f at the D open circles are used to interpolate the function values at the red stars (intersection points of the normal and the vertical grid lines). The values of f at the red points are then used to obtain the values of f at the black points.

4.2.2 Computing continuation values on $V^+_{\theta_p}$

For a given $\theta_p \in \Theta_B$, a continuation of f on $V^+_{\theta_p}$ is obtained via the blending-to-zero algorithm described in Section 4.1. We first obtain the approximations of f on the set $V^-_{\theta_p}$, which are indicated by black solid circles in Figure 4.3, and then using these approximations to obtain a continuation of f via the 1D blending-to-zero procedure along the corresponding normal direction. The values of f on $V^-_{\theta_p}$ are obtained by a two-step polynomial interpolation scheme, using polynomials of degree $D-1$. This is briefly described as follows:

Consider the case where $|n_x(\theta_p)| \geq |n_y(\theta_p)|$. We first estimate the values of f at each red point, which is the intersection of the normal line and the vertical Cartesian grid lines as shown in Figure 4.3, by interpolating vertically the function values at the selected D Cartesian points, shown as open circles, onto the red points. Then we interpolate the values of f at the D red points onto the black solid circles, using a polynomial of degree $D-1$.

The case where $|n_x(\theta_p)| < |n_y(\theta_p)|$ is handled in a similar way by replacing the interpolation along vertical Cartesian grid lines with interpolation along horizontal Cartesian grid lines to obtain the function values at the red points, and then interpolating the function values at the red points onto the black solid points.

4.2.3 Computing continuation values on the Cartesian grid

Once all the continuation values have been obtained on $V^+_{\Theta_B} = \{V^+_{\theta_p}, \theta_p \in \Theta_B\}$, we then obtain the continuation of f on the Cartesian grid points within V^+ using a two-step 1D polynomial interpolation scheme. The 2D-FC algorithm is then completed by evaluating corresponding FCs in (4.2) by means of 2D FFT. The description of the two-step 1D polynomial interpolation scheme is presented below.

For an arbitrary Cartesian point $Q \in \mathcal{H} \cap V^+$, we first obtain the nearest boundary parameter value, θ_p, around Q using a proximity map. This proximity map can be obtained by associating with each curvilinear discretization point $s_{p,q}$ the nearest Cartesian point using *round* operator (which rounds x and y coordinates of Q to the nearest integer), resulting in a set $P_0 \subseteq (\mathcal{H} \cap V^+) \times V^+_{\Theta_B}$ of pairs of points. The set P_0 is then modified by removing multiple associations for a given Cartesian point, and, by adding a next nearest curvilinear neighbor to the Cartesian points that are unassociated.

The algorithm then uses the D-nearest boundary parameter values

$$S_{\theta_p} = \{\theta_{p-K_l}, \theta_{p-K_l+1}, \ldots, \theta_p, \theta_{p+1}, \ldots, \theta_{p+K_r}\},$$

around θ_p (where $K_l + K_r + 1 = D$) to obtain the continuation of f at Q. Parameter values θ_k with negative values of k are interpreted by periodicity: $\theta_k = \theta_{B+k}$.

For each parameter value $\theta_j,\ p - K_l \leq j \leq p + K_r$, we find the signed perpendicular distance from point Q to the normal vector $n(\theta_j)$, denoted by τ_j in Figure 4.4a. Let b_j be the perpendicular projection of Q onto the normal vector $n(\theta_j)$, denoted as the blue points in Figure 4.4. Define

$$\mathcal{T}(\tau_j) = f^c(b_j),\ p - K_l \leq j \leq p + K_r,$$

where $f^c(b_j)$ is the continuation of f at b_j obtained via a 1D polynomial interpolation on D blending to zero points along $n(\theta_j)$ (see Figure 4.4b). Clearly, $\mathcal{T}(0) = f^c(Q)$. It then follows that a 1D polynomial interpolation procedure on the function $\mathcal{T}(\tau)$, using polynomial of degree $D - 1$, can be used to obtain the desired continuation of f at Cartesian point Q.

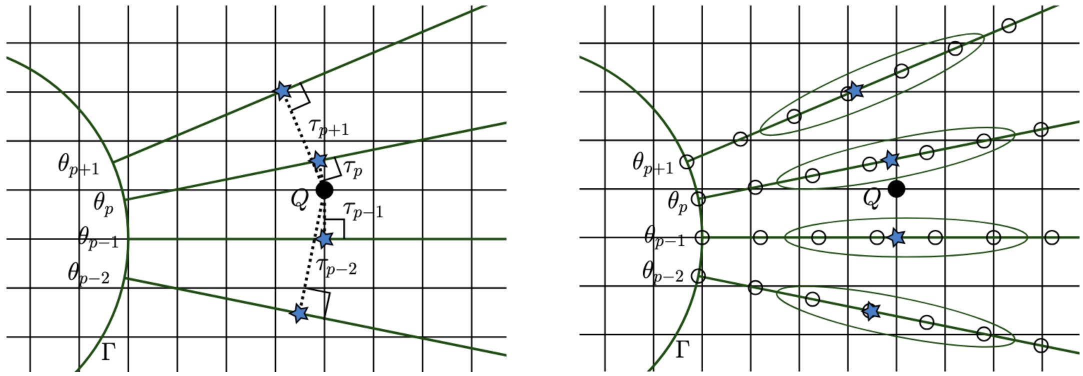

(a) (b)

Figure 4.4: Interpolation procedure for obtaining continuation values of f on $\mathcal{H} \cap V^+$. In (a), the blue-star interpolation points are the perpendicular projections of the Cartesian point Q onto the normal vectors, and the τ's are the perpendicular distances from Q to each normal vector. In (b), the interpolation of continuation values from the curvilinear grids to a point Q on the Cartesian grids.

Finally, by applying a 2D FFT to the continuation function values computed above, we obtain the desired Fourier series expression in (4.2) for the continuation function.

4.2.4 Parameter description and selection

Here, we briefly describe the parameters used in the 2D-FC algorithm. Additionally, we select some specific values for these parameters to get the best result.

- d: number of near-boundary points used to blend f to zero along each normal.
- C: number of continuation points (subsection 4.1).
- k_1: normal step size (subsection 4.2.1).
- k_2: boundary step size (subsection 4.2.1).
- h: step size used to construct Cartesian grid $\mathcal{H}$ (subsection 4.2.1).
- n_r: refinement factor used to obtain the curvilinear grids along each normal vector.
- $N = N_x \times N_y$: number of points in the uniform Cartesian grid (subsection 4.2.1).
- B: number of boundary discretization points (subsection 4.2.1)

- $D-1$: the degree of the interpolating polynomial (subsections 4.2.2 and 4.2.3).

For a given step size h used to construct the Cartesian grid $\mathcal{H}$, we choose normal step size k_1 and boundary step size k_2 to coincide with h. The parameters $C = 25$, $M = 25$, $W = 29$, $\alpha = \beta = 0.15$, and $n_r = 6$ were used in the 1D blending to zero procedure described in Section 4.1. Finally, we set the interpolating polynomial degree $(D-1) = d$ for all matching point numbers d considered except the interpolation-degree experiments presented in Example 1.

In the following example, we demonstrate the performance of the 2D-FC method using three interpolation degrees: $D-1 = d$, $d+1$, and $d+2$ for a given matching point number d.

Example 1. *We consider the FC approximation of the function $f : \Omega \to \mathbb{R}$ given by*

$$f(x, y) = -(x^8 + y^8)\sin(8\pi x)\sin(8\pi y) \tag{4.4}$$

on the unit disk $\Omega = \{(x, y) : x^2 + y^2 \leq 1\}$ with three different values of d: $d = 4$, 5, and 8; and three different values of D: $D = d+1$, $d+2$, and $d+3$.

Figure 4.5 displays the relative L^2 errors as functions of the number of spatial discretization, N_{1D} ($N_x = N_y \approx N_{1D} + 2C$), in one direction within Ω. The errors are computed on a Cartesian grid of step size $h/2$ within Ω. The approximations of f on the finer grid are obtained by means of zero padding [29]. For the case $D = d+1$ (Figure 4.5a), we observe fifth, sixth, and ninth orders of convergence for $d = 4$, 5, and 8 respectively, showing convergence of order $d+1$. However, for the case $D = d+2$ (Figure 4.5b), we observe order $d+2$ convergence for $d = 5$ and 8, and order $d+1$ convergence for $d = 4$. For the case $D = d+3$ (Figure 4.5c), we observe order $d+1$ convergence for $d = 4$ and 5, and order $d+2$ convergence for $d = 8$. The case $D = d+1$, which gives a similar order of convergence $(d+1)$ for the three values of d considered, will be used in all of the numerical experiments presented in this work.

In the next example, we demonstrate the 2D-FC expansion of a two-dimensional non-periodic function defined on a two-dimensional domain contained within the curve given

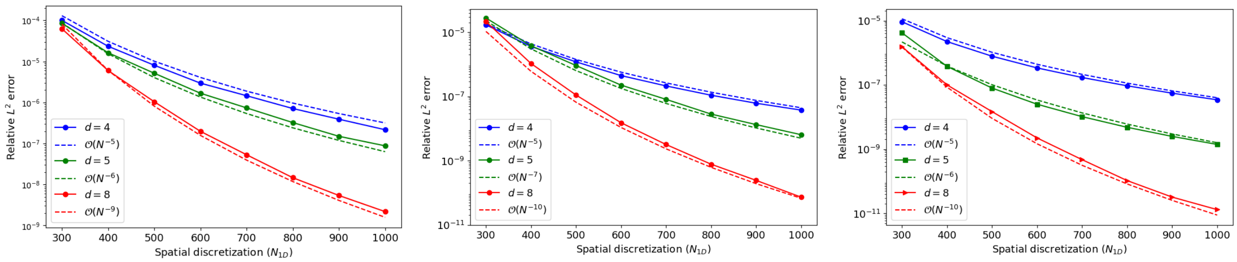

(a) $D = d + 1$ (b) $D = d + 2$ (c) $D = d + 3$

Figure 4.5: Convergence study for the 2D-FC approximation of the function f in (4.4) with three choices of matching point numbers d: $d = 4$, 5, and 8; and three choices of D: $D = d+1$, $d+2$, and $d+3$. The integer N_{1D} is the number of spatial grid points in one spatial direction within Ω.

by

$$x(\theta) = r(\theta)\cos(\theta); \;\; y(\theta) = r(\theta)\sin(\theta), \tag{4.5}$$

where $r(\theta) = 5 + \cos(7\theta)/2 + \sin(4\theta)/3$ and $0 \leq \theta \leq 2\pi$.

Example 2. *We choose $d = 4$, $D = 5$, $h = 0.01$, and employ the 2D-FC method to extend*

$$g(x, y) = 6 + 0.5y - 0.2(x + 1)^2 + 0.6\sin(4.1\sqrt{x^2 + y^2})\cos(3.8(x - y)),$$

over the domain defined in (4.5). Figure 4.6 displays both the original function and its extension.

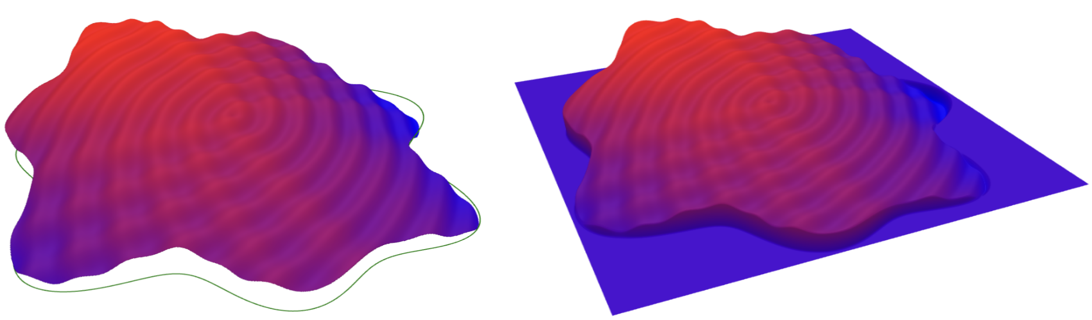

(a) (b)

Figure 4.6: Demonstration of the 2D-FC expansion of a nonperiodic function defined on a 2D domain in the settings of Example 2. (a) the original nonperiodic function g. The green curve indicates the boundary of the domain. (b) the 2D-FC expansion of the function g.

Chapter 5

Fourier spectral method for nonlocal equations on bounded domains

In this chapter, we present a spectral numerical method for solving two-dimensional nonlocal equations on bounded domains. In particular, we solve nonlocal Poisson and nonlocal diffusion equations within bounded domains. Spectral methods are accurate and efficient for solving nonlocal equations because they transform the integral in the nonlocal formulation to multiplication in Fourier space. For example, the application of the nonlocal operator $\mathcal{L}^{\delta,\beta}$ on a function u results in multiplication in Fourier space, as shown in (1.3), and this runs at a computational cost of $\mathcal{O}(N \log N)$ for an N-point discretization grid. For comparison of the efficiency and accuracy of spectral methods versus standard numerical methods such as finite differences, see [1]. A spectral method for nonlocal equations on periodic domains has been developed in [1] with high accuracy, but one difficulty that arises in adapting this spectral method to solve nonlocal equations on bounded domains is that the solutions are in general nonperiodic, therefore exhibiting the Gibbs phenomenon as the Fourier coefficients of the solution decay slowly. One way around this is to use Fourier continuation. The idea behind Fourier continuation is to reduce the impact of slowly decaying Fourier coefficients of a smooth but nonperiodic function on a given domain by constructing a smooth periodic extension of the function over a larger domain. Our proposed solvers build on the Fourier spectral method developed in [1] for the periodic case and the two-dimensional Fourier continuation (2D-FC) method presented in Chapter 4 to solve two-dimensional nonlocal equations within a bounded domain Ω and with Dirichlet conditions on the collar region. The collar region is the extension of Ω by δ and it is defined by

$$\Omega_I = \{\mathbf{y} \in \mathbb{R}^2 \setminus \Omega : \|\mathbf{x} - \mathbf{y}\| \leq \delta, \text{ for some } \mathbf{x} \in \Omega\}.$$

A description of our proposed method is given in the following sections.

5.1 Nonlocal Poisson equation

Consider the following two-dimensional nonlocal Poisson equation with Dirichlet conditions on the collar region

$$\begin{cases} \mathcal{L}^{\delta,\beta} u(x,y) = f(x,y), & (x,y) \in \Omega \\ u(x,y) = b(x,y), & (x,y) \in \Omega_I \end{cases}. \tag{5.1}$$

Our approach for solving (5.1) builds on the spectral method for nonlocal Poisson equation on periodic domains by constructing a periodic extension of the problem using the Fourier continuation algorithm. We then solve the extended problem using the iterative linear algebra solver GMRES [30] to obtain the solution within a specified tolerance. This process is detailed below.

We first transform (5.1) into the following linear system

$$Au = g, \quad A = \begin{pmatrix} L \\ B \end{pmatrix}, \quad g = \begin{pmatrix} f \\ b \end{pmatrix}, \tag{5.2}$$

where L and B are respectively the associated matrices of the nonlocal operator $\mathcal{L}^{\delta,\beta}$ and the boundary operator $\mathcal{B}$ given by the Dirichlet conditions on the collar region. To apply

GMRES to this system, we do not need to compute A and store it in memory. Instead, it is sufficient to express the forward operator $v \mapsto Av$ as a function. The action of the operator $\mathcal{B}$ is a restriction of the values of v to the collar region. We derive the forward operator function using the properties of $\mathcal{L}^{\delta,\beta}$ as follows:

$$u \to u_{\text{ext}} \to \widehat{u}_{\text{ext}} \to \widehat{Lu_{\text{ext}}} = m^{\delta,\beta}\widehat{u}_{\text{ext}} \to Lu_{\text{ext}} \to Lu, \tag{5.3}$$

where u_{ext} is the extension of u obtained by the 2D-FC method, $\widehat{u}_{\text{ext}}$ is the Fourier transform of u_{ext} obtained by means of the fast Fourier transform (FFT), Lu_{ext} is the inverse Fourier transform of $\widehat{Lu_{\text{ext}}}$, and Lu is the restriction of Lu_{ext} to the domain Ω. We then obtain the solution of (5.1) by applying GMRES to the system (5.2) within a specified tolerance.

5.2 Nonlocal diffusion equation

Consider the following 2D nonlocal diffusion equation with Dirichlet conditions on the collar region and with initial condition

$$\begin{cases} u_t(x,y,t) = \mathcal{L}^{\delta,\beta}u(x,y,t) + s(x,y,t), & (x,y,t) \in \Omega \times (0,T), \\ u(x,y,0) = u_0(x,y), & (x,y) \in \Omega, \\ u(x,y,t) = b(x,y), & (x,y) \in \Omega_I. \end{cases} \tag{5.4}$$

Similar to the nonlocal Poisson solver, we first construct the periodic extension of (5.4) using the 2D-FC algorithm. We then solve the extended problem using the fourth-order Adams-Bashforth method. The process is detailed below.

First, consider the semi-discrete form of (5.4), where we replace u by a time dependent vector $\vec{u}$ as follows

$$\vec{u}' = \mathcal{L}^{\delta,\beta}\vec{u} + \vec{s} := f(\vec{u}). \tag{5.5}$$

For a given final time $T > 0$ and a time step-size τ, we first obtain the vectors $\vec{u}_1$, $\vec{u}_2$, and $\vec{u}_3$, using the fourth-order Runge-Kutta method. Then, for $k = 4, 5, \dots, K$, where $K = T/\tau$, we obtain $\vec{u}_k$ by using the fourth-order Adams-Bashforth method given by

$$\vec{u}_{k+4} = \vec{u}_{k+3} + \tau \left(\frac{55}{24} f(\vec{u}_{k+3}) - \frac{59}{24} f(\vec{u}_{k+2}) + \frac{37}{24} f(\vec{u}_{k+1}) - \frac{9}{24} f(\vec{u}_k) \right).$$

To obtain $f(\vec{u}_k)$, $k = 0, 1, \dots, K$, we apply the 2D-FC method to extend $\vec{u}$ in (5.5), as follows

$$\vec{u}_k \to (\vec{u}_k)_{\text{ext}} \to \widehat{(\vec{u}_k)}_{\text{ext}} \to (\widehat{\mathcal{L}^{\delta,\beta}\vec{u}_k})_{\text{ext}} = m^{\delta,\beta}\widehat{(\vec{u}_k)}_{\text{ext}} \to (\mathcal{L}^{\delta,\beta}\vec{u}_k)_{\text{ext}} \to \mathcal{L}^{\delta,\beta}\vec{u}_k + \vec{s}_k = f(\vec{u}_k),$$

where $(\vec{u}_k)_{\text{ext}}$ is the extension of $\vec{u}_k$ obtained by the 2D-FC method, $\widehat{(\vec{u}_k)}_{\text{ext}}$ is the Fourier transform of $(\vec{u}_k)_{\text{ext}}$ obtained by means of FFT, $(\mathcal{L}^{\delta,\beta}\vec{u}_k)_{\text{ext}}$ is the inverse Fourier transform of $(\widehat{\mathcal{L}^{\delta,\beta}\vec{u}_k})_{\text{ext}}$, and $\mathcal{L}^{\delta,\beta}\vec{u}_k$ is the restriction of $(\mathcal{L}^{\delta,\beta}\vec{u}_k)_{\text{ext}}$ to the domain Ω.

5.3 Numerical results

This section demonstrates the accuracy and performance of our proposed method for solving nonlocal equations on bounded domains. In particular, we present the convergence study for the spectral solvers described in Sections 5.1 and 5.2 for the 2D nonlocal Poisson and nonlocal diffusion equations, respectively. Additionally, we study the discontinuities in the solutions of these equations. The 2D-FC parameters are as chosen in Section 4.2.4.

5.3.1 Convergence test for nonlocal Poisson equation

Here, we construct a manufactured solution to study the accuracy and convergence of the nonlocal Poisson equation (5.1). To this end, let

$$u(x, y) = \sin(2\pi r_1 x)\sin(2\pi r_2 y)$$

δ	β=1.2 $m^{\delta,\beta}$	β=2.0 $m^{\delta,\beta}$	β=2.5 $m^{\delta,\beta}$
0.4	−82.87098585883194	−180.5053934013443	−387.0397711705603

Table 5.1: The multipliers of the nonlocal operator $\mathcal{L}^{\delta,\beta}$ applied on $u = \sin(2\pi r_1 x)\sin(2\pi r_2 y)$, where $r_1 = 10.6418$ and $r_2 = 12.6418$, with a fixed $\delta = 0.4$ and three different values of β.

be the solution of (5.1), where $r_1 = 10.6418$ and $r_2 = 12.6418$. Clearly, $u(x, y)$ is a highly oscillatory nonperiodic function. To obtain the right hand side function, $f(x, y)$, we apply the operator $\mathcal{L}^{\delta,\beta}$ on u, using the property of $\mathcal{L}^{\delta,\beta}$ given in (1.3), with fixed $\delta = 0.4$ and three different values of β : 1.2, 2.0, and 2.5. These values of β represents $\beta < n$, $\beta = n$, and $\beta > n$. A direct computation of the multipliers $m^{\delta,\beta}$ is provided in Table 5.1. We compute these multipliers using the implementation of the ${}_2F_3$ hypergeometric function provided by mpmath [31], as detailed in [17]. We then use these manufactured solutions to compute the errors as shown in the following example.

Example 3 (Convergence test for the nonlocal Poisson equation)**.** *We employ our proposed spectral method to solve the nonlocal Poisson equation* (5.1) *over the unit disk and study the error convergence using eight numbers of spatial discretizations* $N_x = N_y = 300, 400, 500, 600, 700, 800, 900,$ *and* 1000. *We fix* $\delta = 0.4$*, and choose three different values of* β : 1.2*,* 2.0*,* 2.5*. We set the boundary function* $b(x, y) = \sin(2\pi r_1 x)\sin(2\pi r_2 y)$ *and the right-hand side function*

$$f(x, y) = \mathcal{L}^{\delta,\beta} b(x, y) = m^{\delta,\beta} b(x, y),$$

where $r_1 = 10.6418$*,* $r_2 = 12.6418$*, and the multipliers* $m^{\delta,\beta}$ *are as given in Table 5.1.*

A convergence study for this test case is shown in Figure 5.1 for $d = 4$ and $d = 5$, with fixed $D = d + 1$. We use the manufactured solution described above to compute the L^2 errors reported. We observe seventh and eighth orders of convergence for $d = 4$ and $d = 5$, respectively, showing convergence of order $d + 3$ for the three cases of β considered.

Moreover, we observe no significant difference in the errors reported for $d = 4$ and $d = 5$

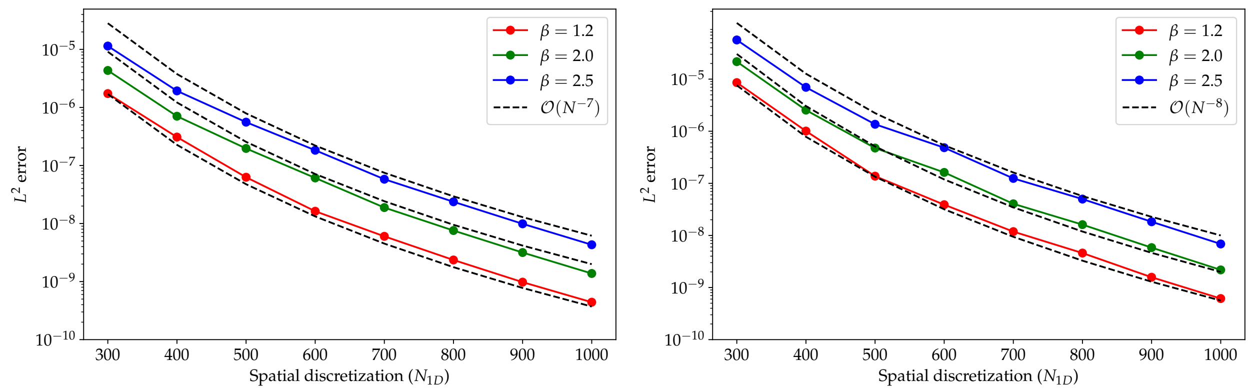

(a) $d = 4$ (b) $d = 5$

Figure 5.1: Convergence of the 2D-FC based solution of the nonlocal Poisson equation (5.1) in the settings of Example 3 with fixed $\delta = 0.4$, fixed $D = d + 1$, and two values of d.

for these numbers of spatial discretizations. Thus, for the rest of this work, we will use $d = 4$ for all numerical computations of nonlocal Poisson equations.

5.3.2 Convergence test for nonlocal diffusion equation

Similarly, we construct a manufactured solution to study the accuracy and convergence for the nonlocal diffusion equation (5.4). Let

$$u(x, y, t) = e^{-2\pi^2 \kappa t} \sin(2\pi r_1 x) \sin(2\pi r_2 y)$$

be the solution of (5.4), where $\kappa = 0.1$, $r_1 = r_2 = 15.6455$. Clearly, $u(x, y)$ is highly oscillatory and nonperiodic. To obtain the heat source, $s(x, y, t)$, we apply operator $\mathcal{L}^{\delta,\beta}$ on u, using the property of $\mathcal{L}^{\delta,\beta}$ given in (1.3), with fixed $\delta = 0.2$ and three values of β : 1.0, 2.0, and 2.5. Thus,

$$s(x, y, t) = u_t - \mathcal{L}^{\delta,\beta} u = \left(-2\pi^2 \kappa - m^{\delta,\beta}\right) u. \tag{5.6}$$

A direct computation of the multipliers $m^{\delta,\beta}$ is provided in Table 5.2. We compute these multipliers using the implementation of the ${}_2F_3$ hypergeometric function provided by mpmath [31], as detailed in [17].

Example 4 (Convergence test for nonlocal diffusion equation)**.** *We employ our proposed*

δ	$\overset{\beta=1.0}{m^{\delta,\beta}}$	$\overset{\beta=2.0}{m^{\delta,\beta}}$	$\overset{\beta=2.5}{m^{\delta,\beta}}$
0.3	−130.16228859689554	−321.3202730766787	−689.8419741563309

Table 5.2: The multipliers of the nonlocal operator $\mathcal{L}^{\delta,\beta}$ applied on $u = \sin(2\pi r_1 x)\sin(2\pi r_2 y)$, where $r_1 = r_2 = 15.6455$, with a fixed $\delta = 0.3$ and three different values of β.

method to study the error convergence of the nonlocal diffusion problem (5.4) *over the kite-shaped domain contained within the curve given by*

$$x(\theta) = \cos(\theta) + 0.35\cos(\theta) - 0.35;\ y(\theta) = 0.7\sin(\theta) \quad \textit{for } 0 \leq \theta \leq 2\pi \tag{5.7}$$

using step sizes $h = 0.02/2^k$, $k = 0, 1, 2, 3, 4$ *and time step size* $\tau = 5.0 \cdot 10^{-07}$. *We fix* $\delta = 0.3$, *and choose three values of* β : 1.0, 2.0, *and* 2.5, *and we set the boundary function* $b(x, y) = e^{-2\pi^2\kappa t}\sin(2\pi r_1 x)\sin(2\pi r_2 y)$, *where* $\kappa = 0.1$, $r_1 = r_2 = 15.6455$, *and the heat source,* $s(x, y, t)$, *is as given in* (5.6).

A convergence study for this test case is shown in Table 5.3 for $d = 4$ and $d = 5$, with fixed $D = d + 1$. We use the manufactured solution described above to compute the L^2 errors reported. We observe sixth and seventh orders of convergence for $d = 4$ and $d = 5$, respectively, showing convergence of order $d + 2$ for the three cases of β considered.

Moreover, as observed in the case of nonlocal Poisson equation, we observe no significant difference in the errors reported for $d = 4$ and $d = 5$. Thus, for the rest of this work, we will use $d = 4$ for all numerical computations of nonlocal diffusion equations.

5.3.3 Study of discontinuities for the nonlocal Poisson equation

In this section, we study the behavior of the discontinuities in the numerical solutions of nonlocal Poisson equations on bounded domains. For the case of integrable kernels ($\beta < 2$), we emphasize that if f is discontinuous, then the solution of the nonlocal Poisson equation is also discontinuous and will share the same location of jumps with f. However, for the case of singular kernels with $\beta > 3$, we form a conjecture that even if f is discontinuous, the

d	h	$\varepsilon_2^{\beta=1.0}$	Order	$\varepsilon_2^{\beta=2.0}$	Order	$\varepsilon_2^{\beta=2.5}$	Order
4	$2.00 \cdot 10^{-2}$	$1.13 \cdot 10^{-05}$	—	$5.33 \cdot 10^{-05}$	—	$2.48 \cdot 10^{-04}$	—
	$1.00 \cdot 10^{-2}$	$1.51 \cdot 10^{-07}$	6.2	$9.45 \cdot 10^{-07}$	5.8	$6.81 \cdot 10^{-06}$	5.2
	$5.00 \cdot 10^{-3}$	$2.07 \cdot 10^{-09}$	6.2	$1.48 \cdot 10^{-08}$	6.0	$1.45 \cdot 10^{-07}$	5.6
	$2.50 \cdot 10^{-3}$	$1.87 \cdot 10^{-11}$	6.8	$9.21 \cdot 10^{-11}$	7.3	$1.22 \cdot 10^{-09}$	6.9
	$1.25 \cdot 10^{-3}$	$2.43 \cdot 10^{-13}$	6.3	$1.29 \cdot 10^{-12}$	6.2	$2.29 \cdot 10^{-11}$	5.7
5	$2.00 \cdot 10^{-2}$	$7.87 \cdot 10^{-05}$	—	$4.10 \cdot 10^{-04}$	—	$1.93 \cdot 10^{-03}$	—
	$1.00 \cdot 10^{-2}$	$8.84 \cdot 10^{-07}$	6.5	$5.86 \cdot 10^{-06}$	6.1	$4.16 \cdot 10^{-05}$	5.5
	$5.00 \cdot 10^{-3}$	$5.53 \cdot 10^{-09}$	7.3	$3.30 \cdot 10^{-08}$	7.5	$3.23 \cdot 10^{-07}$	7.0
	$2.50 \cdot 10^{-3}$	$2.99 \cdot 10^{-11}$	7.5	$1.87 \cdot 10^{-10}$	7.5	$2.49 \cdot 10^{-09}$	7.0
	$1.25 \cdot 10^{-3}$	$3.49 \cdot 10^{-13}$	6.4	$1.27 \cdot 10^{-12}$	7.2	$2.15 \cdot 10^{-11}$	6.9

Table 5.3: Convergence of the 2D-FC based solution of the nonlocal diffusion equation (5.4) in the settings of Example 4 with fixed $\delta = 0.3$, fixed $D = d + 1$, two different values of d: 4 and 5, and three choices of β: 1.0, 2.0, and 2.5.

solution will be continuous.

Example 5. *Let Ω be the kite-shaped domain contained within the curve defined in (5.7). We solve the nonlocal Poisson equation (5.1) over Ω using $h = 0.0025$ with $\delta = 0.4$, and three different values of β : 1.0, 2.0, and 3.0, and we set $f(x, y) = 4$ and $b(x, y) = x^2 + y^2$.*

In Figure 5.2, we observe that the solutions are continuous everywhere and are the same for the three cases of β considered. This continuity arises from the fact that the nonlocal Laplace operator behaves like the classical Laplace operator when applied on any polynomial of degree ≤ 2 for any value of β or δ. Since the boundary function $b(x, y)$ is a polynomial of degree 2, and $f(x, y) = 4$, then the solution $u(x, y)$ must also be a polynomial of degree 2, which is continuous everywhere.

Example 6. *Let Ω be the unit disk. We solve the nonlocal Poisson equation (5.1) over Ω with $h = 0.0025$. We choose $\delta = 0.2$, three values of β : 1.5, 2.2, 3.1, and we set $f(x, y) = |\sin(\pi x)\sin(\pi y)|$ and $b(x, y) = -x^2$.*

Figure 5.3 presents the numerical solution for the three choices of β considered. We observe that the solution is discontinuous at $\partial\Omega$, and the magnitude of the jump decreases as β increases. Specifically, we observe that for $\beta > 3$, the magnitude of the jump is small.

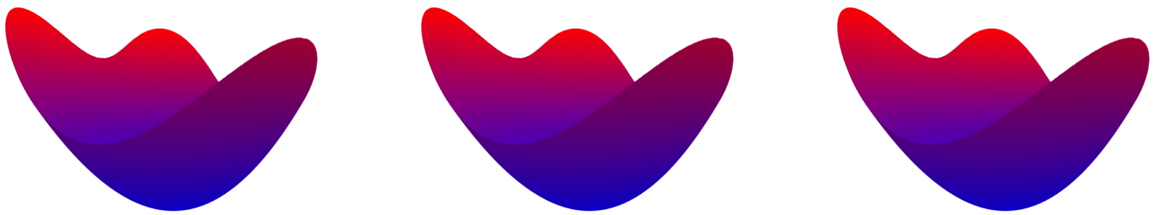

(a) $\beta = 1.0$ (b) $\beta = 2.0$ (c) $\beta = 3.0$

Figure 5.2: Simulation results in Example 5 with a fixed $\delta = 0.4$ and three choices of β.

The maximum and the minimum magnitudes of the jumps at $\partial\Omega$ for all the values of β considered are provided in Table 5.4, and they are computed using the following formula:

$$\text{magnitude of the jump} = \left|\widetilde{u}(x_\theta, y_\theta) - b(x_\theta, y_\theta)\right|,$$

where $\widetilde{u}$ is the extension of u from the interior of Ω to the boundary $\partial\Omega$, x_θ and y_θ are the x and y coordinates of the boundary $\partial\Omega$ at $\theta \in \Theta_B$, and b is the given boundary function.

	$\beta = 1.5$	$\beta = 2.2$	$\beta = 3.1$
min magnitude	0.0538468	0.0187264	$6.24 \cdot 10^{-05}$
max magnitude	0.0646947	0.0372901	0.0097378

Table 5.4: The minimum and the maximum magnitudes of the jumps at $\partial\Omega$ in the simulations results presented in Figure 5.3. We observe that the magnitudes of the jumps decrease as β increases.

The following example considers the case where $f(x, y)$ is discontinuous. As in the periodic case, we expect the solution to be discontinuous at the location where f is discontinuous.

Example 7. *Let Ω be the kite-shaped domain contained within the curve defined in (5.7). We solve the nonlocal Poisson equation (5.1) over Ω with $h = 0.0025$. We choose $\delta = 0.5$, four different values of β : 1.2, 2.0, 2.5, 3.1, and we set the boundary function $b(x, y) = x^2 + y^2$ and*

$$f(x, y) = \begin{cases} 80, & \text{if } x^2 + 4y^2 < 0.2 \\ 4, & \text{otherwise} \end{cases}.$$

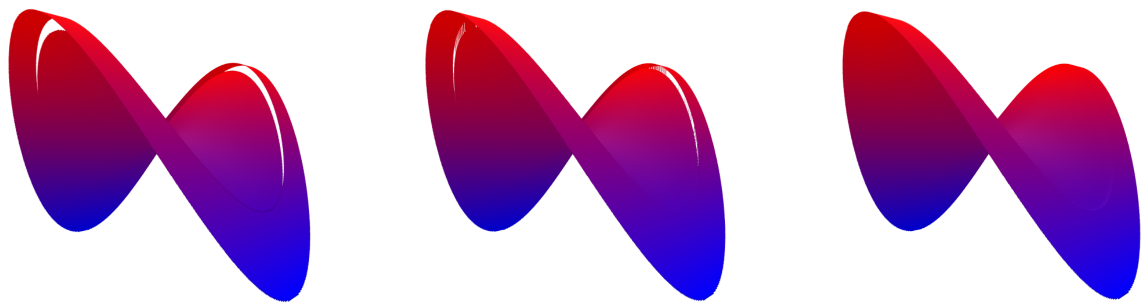

(a) $\beta = 1.5$ (b) $\beta = 2.2$ (c) $\beta = 3.1$

Figure 5.3: Simulation results in Example 6 with a fixed $\delta = 0.2$ and three different values of β. We observe that the magnitude of the jump at the $\partial\Omega$ decreases as β increases (see Table 5.4).

In Figure 5.4, we present the numerical solutions for four different values of β: 1.2, 2.0, 2.5, and 3.1. We observe that as β increases, the magnitudes of the jump discontinuity inside the domain Ω and at its boundary $\partial\Omega$ decrease. Furthermore, these discontinuities occur at the exact location where f is discontinuous. Specifically, the maximum and the minimum magnitudes of the jumps in the interior of the domain for all the values of β considered are given in Table 5.5, and they are computed using the following formula:

$$\text{magnitude of the jump} = \left|\widetilde{u}_{\text{int}}(x_\theta, y_\theta) - \widetilde{u}_{\text{ext}}(x_\theta, y_\theta)\right|,$$

where $\widetilde{u}_{\text{int}}$ is the extension of u from the interior of the ellipse to the boundary of the ellipse, $\widetilde{u}_{\text{ext}}$ is the extension of u from the exterior of the ellipse to the boundary of the ellipse, and x_θ and y_θ are the x and y coordinates of the boundary of the ellipse at $\theta \in \Theta_B$.

	$\beta = 1.2$	$\beta = 2.0$	$\beta = 2.5$	$\beta = 3.1$
min magnitude	1.3589861	0.3237825	0.0363031	$1.75 \cdot 10^{-05}$
max magnitude	1.3681906	0.4040726	0.0856388	0.0067363

Table 5.5: The minimum and the maximum magnitudes of the jumps in the interior of Ω in the simulations results presented in Figure 5.4. We observe that the magnitudes of the jumps decrease as β increases..

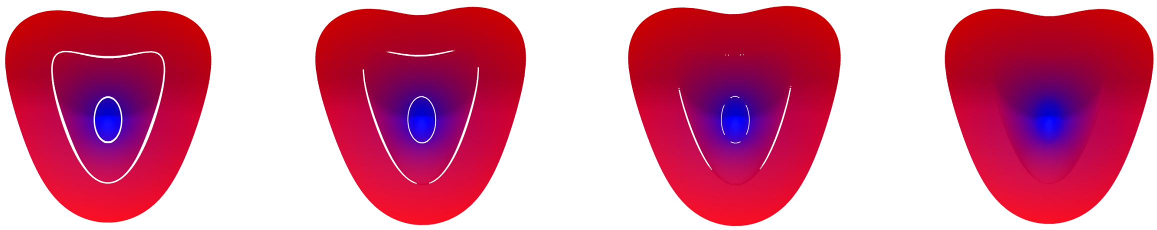

(a) $\beta = 1.2$ (b) $\beta = 2.0$ (c) $\beta = 2.5$ (d) $\beta = 3.1$

Figure 5.4: Simulation results in Example 7 with a fixed $\delta = 0.5$ and four choices of β.

To make a connection between the numerical results in this work, in particular Example 7, and previous mathematical analysis in this area, we note that regularity results for the nonlocal Poisson equation on periodic domains have been developed in [17]. However, regularity of solutions for the nonlocal equation on bounded domains is still an open problem.

For the periodic case, Theorem 4.1 in [17] implies that if $f \in L^2$, then $u \in H^{\beta-n}$. In particular, in the case when when $n = 2$ and $3 < \beta < 4$, then $u \in H^{\beta-2}$, which implies that u is continuous using the embedding theorem. Using intuition from the periodic case combined with the numerical observations in Example 7, we expect that this smoothing behavior as β increases would be true in the case of bounded domains as stated in the following conjecture.

Conjecture 1. *Let u be the solution of (5.1) and assume that $f \in L^2(\Omega)$. Then, if $3 < \beta < 4$, then $u \in C(\Omega)$.*

5.3.4 Evolution of discontinuities for nonlocal diffusion equation

In this section, we study the propagation of discontinuity in the solution of nonlocal diffusion equation (5.4). We emphasize that the nonlocal diffusion equation with nonlocal boundary conditions also satisfies an instantaneous smoothing effect when $\beta > n$, a gradual smoothing effect when $\beta = n$, and non-smoothing when $\beta < n$.

Example 8. *Let Ω be the domain contained within the curve given by*

$$x(\theta) = r(\theta)\cos(\theta); \;\; y(\theta) = r(\theta)\sin(\theta), \tag{5.8}$$

where $r(\theta) = 1.1 + \cos(7t)/20 + \sin(4t)/30$, *and* $0 \leq \theta \leq 2\pi$. *We solve the nonlocal diffusion equation* (5.4) *over* Ω *at four different time instances:* 0.02, 0.03, 0.04, *and* 0.05 *with time step size* $\tau = 2.5 \cdot 10^{-7}$ *and spatial step size* $h = 0.005$. *We set the initial condition* $u_0(x, y) = \sin(2\pi x)\cos(2\pi y)$, *the boundary function* $b(x, y) = -(1 + x^2 + y^2)$, *and the heat source* $s(x, y, t) = 0$.

In this case, the corresponding classical heat equation is given by

$$\begin{cases} u_t(x,y,t) = \Delta u(x,y,t), & (x,y,t) \in \Omega \times (0,T), \\ u(x,y,0) = \sin(2\pi x)\cos(2\pi y), & (x,y) \in \Omega, \\ u(x,y) = -(1 + x^2 + y^2), & (x,y) \in \partial\Omega. \end{cases} \tag{5.9}$$

The first row of Figure 5.5 demonstrates the numerical solution to the classical diffusion problem (5.9) at different times $t = 0.02$, 0.03, 0.04, and 0.05. The second row of Figure 5.5, demonstrates the numerical solution for the nonlocal diffusion problem in Example 8 with fixed $\delta = 0.2$ and $\beta = 1.5$ for the same corresponding times $t = 0.02$, 0.03, 0.04, and 0.05. For classical diffusion, we observe an instantaneous smoothing effect at $\partial\Omega$, in particular, the solution is continuous at the boundary. In contrast, the solution to the nonlocal problem is discontinuous at $\partial\Omega$, however, the magnitude of the jump decreases as time increases. We further observe that for both local and nonlocal diffusion, oscillations in the initial data smooth out as time increases.

Example 9. *We solve the nonlocal diffusion equation* (5.1) *over the domain contained within the curve given in* (5.7) *with spatial step size* $h = 0.005$ *and time step size* $\tau = 2.5 \cdot 10^{-7}$ *at four different time instances:* $t = 0.001$, 0.005, 0.01, *and* 0.03. *We set* $b(x, y) = 0$, *the heat source* $s(x, y, t) = 0$, *and the initial condition*

$$u_0(x,y) = \begin{cases} 2, & \text{if } x^2 + y^2 < 0.3, \\ e^{-x^4 - y^4}, & \text{otherwise.} \end{cases}$$

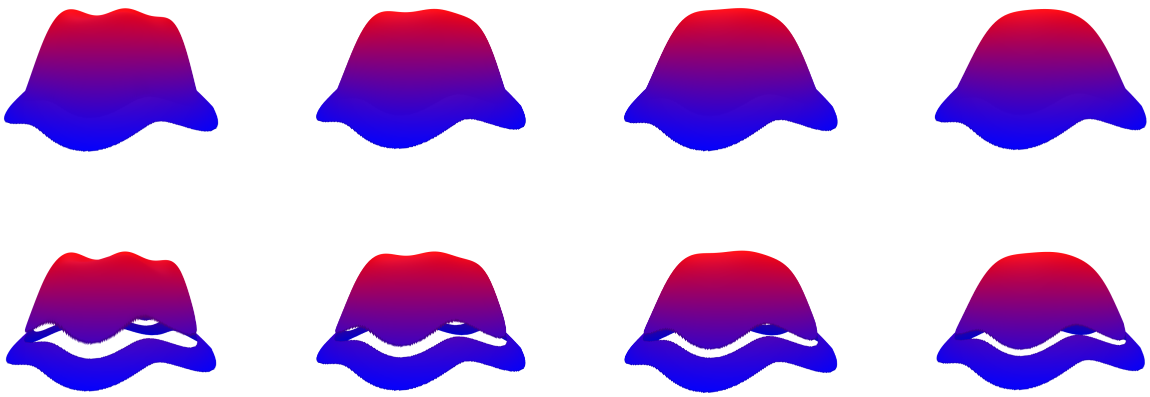

(a) $t = 0.02$ (b) $t = 0.03$ (c) $t = 0.04$ (d) $t = 0.05$

Figure 5.5: Simulation results in Example 8 with fixed $\delta = 0.2$ and two different values of β: 4.0 (first row) and 1.5 (second row) at four different time instances.

In Figure 5.6, we present the numerical solutions for a fixed $\delta = 0.2$ and two values of β: 4.0 and 1.0 at different final time. For the case $\beta = 4.0$, which corresponds to the classical heat equation, we observe an instantaneous smoothing effect at $\partial\Omega$ compared to the nonlocal counterpart where $\beta = 1.0$.

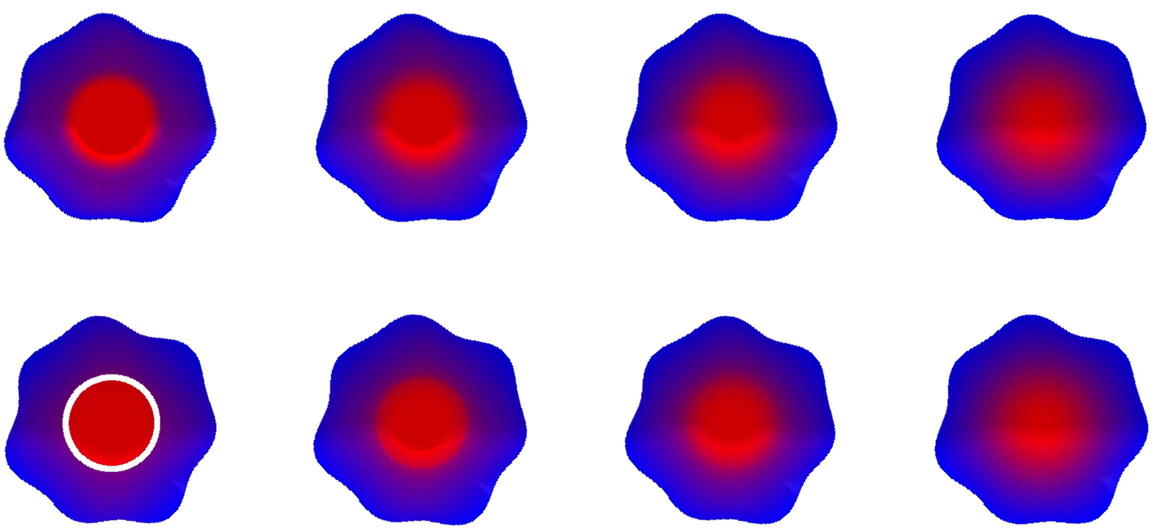

(a) $t = 0.001$ (b) $t = 0.005$ (c) $t = 0.01$ (d) $t = 0.03$

Figure 5.6: Simulation results in Example 9 with fixed $\delta = 0.2$ and two different values of β: 4.0 (first row) and 1.0 (second row) at four different time instances.

Bibliography

[1] Bacim Alali and Nathan Albin. Fourier spectral methods for nonlocal models. *Journal of Peridynamics and Nonlocal Modeling*, 2:317–335, 2020.

[2] Oscar P Bruno and Jagabandhu Paul. Two-dimensional fourier continuation and applications. *SIAM Journal on Scientific Computing*, 44(2):A964–A992, 2022.

[3] Florin Bobaru, John T Foster, Philippe H Geubelle, and Stewart A Silling. *Handbook of peridynamic modeling*. CRC press, 2016.

[4] Mewael Isiet, Ilija Mišković, and Sanja Mišković. Review of peridynamic modelling of material failure and damage due to impact. *International Journal of Impact Engineering*, 147:103740, 2021.

[5] Florin Bobaru and Guanfeng Zhang. Why do cracks branch? a peridynamic investigation of dynamic brittle fracture. *International Journal of Fracture*, 196(1-2):59–98, 2015.

[6] Will Hicks. Nonlocal diffusions and the quantum black-scholes equation: Modelling the market fear factor. *arXiv preprint arXiv:1806.07983*, 2018.

[7] Emma Lejeune and Christian Linder. Modeling tumor growth with peridynamics. *Biomechanics and modeling in mechanobiology*, 16(4):1141–1157, 2017.

[8] Stewart A Silling. Reformulation of elasticity theory for discontinuities and long-range forces. *Journal of the Mechanics and Physics of Solids*, 48(1):175–209, 2000.

[9] Stewart A Silling, M Epton, O Weckner, Ji Xu, and E23481501120 Askari. Peridynamic states and constitutive modeling. *Journal of Elasticity*, 88(2):151–184, 2007.

[10] Q. Du, M. Gunzburger, R. B. Lehoucq, and K. Zhou. A nonlocal vector calculus, nonlocal volume-constrained problems, and nonlocal balance laws. *Mathematical Models and Methods in Applied Sciences*, 23(03):493–540, 2013. doi: 10.1142/S0218202512500546. URL http://www.worldscientific.com/doi/abs/10.1142/S0218202512500546.

[11] Guy Gilboa and Stanley Osher. Nonlocal operators with applications to image processing. *Multiscale Modeling & Simulation*, 7(3):1005–1028, 2009.

[12] T. Mengesha and Q. Du. Nonlocal constrained value problems for a linear peridynamic navier equation. *Journal of Elasticity*, 116(1):27–51, 2014.

[13] Moritz Kassmann, Tadele Mengesha, and James Scott. Solvability of nonlocal systems related to peridynamics. *Communications on Pure & Applied Analysis*, 18(3):1303, 2019.

[14] Mikil Foss and Petronela Radu. Differentiability and integrability properties for solutions to nonlocal equations. In *New Trends in Differential Equations, Control Theory and Optimization: Proceedings of the 8th Congress of Romanian Mathematicians*, pages 105–119. World Scientific, 2016.

[15] Tadele Mengesha and James M Scott. The solvability of a strongly-coupled nonlocal system of equations. *Journal of Mathematical Analysis and Applications*, 486(2):123919, 2020.

[16] Qiang Du, Max Gunzburger, Richard B Lehoucq, and Kun Zhou. Analysis and approximation of nonlocal diffusion problems with volume constraints. *SIAM review*, 54(4): 667–696, 2012.

[17] Bacim Alali and Nathan Albin. Fourier multipliers for nonlocal laplace operators. *Applicable Analysis*, 100(12):2526–2546, 2021.

[18] Brittney Hinds and Petronela Radu. Dirichlet's principle and wellposedness of solutions for a nonlocal p-laplacian system. *Applied Mathematics and Computation*, 219(4):1411–1419, 2012.

[19] Olena Burkovska and Ilyas Mustapha. An efficient proximal-based approach for solving nonlocal allen-cahn equations. *arXiv preprint arXiv:2410.06455*, 2024.

[20] Erdogan Madenci, Erkan Oterkus, Erdogan Madenci, and Erkan Oterkus. Coupling of the peridynamic theory and finite element method. *Peridynamic theory and its applications*, pages 191–202, 2014.

[21] Dennj De Meo and Erkan Oterkus. Finite element implementation of a peridynamic pitting corrosion damage model. *Ocean Engineering*, 135:76–83, 2017.

[22] Qiang Du and Jiang Yang. Asymptotically compatible fourier spectral approximations of nonlocal allen–cahn equations. *SIAM Journal on Numerical Analysis*, 54(3):1899–1919, 2016.

[23] Siavash Jafarzadeh, Adam Larios, and Florin Bobaru. Efficient solutions for nonlocal diffusion problems via boundary-adapted spectral methods. *Journal of Peridynamics and Nonlocal Modeling*, 2:85–110, 2020.

[24] Qiang Du and Jiang Yang. Fast and accurate implementation of fourier spectral approximations of nonlocal diffusion operators and its applications. *Journal of Computational Physics*, 332:118–134, 2017.

[25] Richard Mikaël Slevinsky, Hadrien Montanelli, and Qiang Du. A spectral method for nonlocal diffusion operators on the sphere. *Journal of Computational Physics*, 372: 893–911, 2018.

[26] Nathan Albin and Oscar P Bruno. A spectral fc solver for the compressible navier–stokes equations in general domains i: Explicit time-stepping. *Journal of Computational Physics*, 230(16):6248–6270, 2011.

[27] Loukas Grafakos. *Classical fourier analysis*, volume 2. Springer, 2008.

[28] Nathan Albin and Sureka Pathmanathan. Discrete periodic extension using an approximate step function. *SIAM Journal on Scientific Computing*, 36(2):A668–A692, 2014.

[29] William H Press, Saul A Teukolsky, William T Vetterling, and Brian P Flannery. Numerical recipes 3rd edition. *The art of scientific computing*, 3, 2007.

[30] Yousef Saad. *Iterative methods for sparse linear systems*. SIAM, 2003.

[31] Fredrik Johansson et al. mpmath: a python library for arbitrary-precision floating-point arithmetic (version 0.18). *Official Wiki Page available at: http://code.google.com/p/mpmath*, 2013.